



**Calhoun: The NPS Institutional Archive**  
**DSpace Repository**

---

Theses and Dissertations

1. Thesis and Dissertation Collection, all items

---

1995-06

# Development of ground support equipment for the NPS Ionospheric Spectroscopy and Atmospheric Chemistry (ISAAC) Ultraviolet Spectrograph

Leloudas, Fragiskos.

Monterey, California. Naval Postgraduate School

---

<http://hdl.handle.net/10945/7509>

---

This publication is a work of the U.S. Government as defined in Title 17, United States Code, Section 101. Copyright protection is not available for this work in the United States.

*Downloaded from NPS Archive: Calhoun*



<http://www.nps.edu/library>

Calhoun is the Naval Postgraduate School's public access digital repository for research materials and institutional publications created by the NPS community. Calhoun is named for Professor of Mathematics Guy K. Calhoun, NPS's first appointed -- and published -- scholarly author.

**Dudley Knox Library / Naval Postgraduate School**  
**411 Dyer Road / 1 University Circle**  
**Monterey, California USA 93943**

**NAVAL POSTGRADUATE SCHOOL**  
**Monterey, California**



**THESIS**

**DEVELOPMENT OF GROUND SUPPORT  
EQUIPMENT FOR THE NPS IONOSPHERIC  
SPECTROSCOPY AND ATMOSPHERIC  
CHEMISTRY (ISAAC) ULTRAVIOLET  
SPECTROGRAPH**

by

Fragiskos Leloudas

June 1995

Thesis Advisor:  
Thesis Co-Advisor:

David D. Cleary  
Suntharalingam Gnanalingam

Approved for public release; distribution is unlimited

Thesis  
L47867

DUDLEY KNOX LIBRARY  
NAVAL POSTGRADUATE SCHOOL  
MONTEREY CA 93943-5101

|   |  |   |   |   |
|---|--|---|---|---|
| REPORT DOCUMENTATION PAGE   |  |   | Form Approved<br>OMB No. 0704-0188                  |   |
| Public reporting burden for this collection of information is estimated to average 1 hour per response, including the time for reviewing instruction, searching existing data sources, gathering and maintaining the data needed, and completing and reviewing the collection of information. Send comments regarding this burden estimate or any other aspect of this collection of information, including suggestions for reducing this burden, to Washington headquarters Services, Directorate for Information Operations and Reports, 1215 Jefferson Davis Highway, Suite 1204, Arlington, VA 22202-4302, and to the Office of Management and Budget, Paperwork Reduction Project (0704-0188) Washington DC 20503.   |  |   |   |   |
| 1. AGENCY USE ONLY (Leave blank)  |  | 2. REPORT DATE<br>June 1995                                 |   | 3. REPORT TYPE AND DATES COVERED<br>Master's Thesis |
| 4. TITLE AND SUBTITLE<br>DEVELOPMENT OF GROUND SUPPORT EQUIPMENT FOR THE NPS<br>IONOSPHERIC SPECTROSCOPY AND ATMOSPHERIC CHEMISTRY<br>(ISAAC) ULTRAVIOLET SPECTROGRAPH  |  |   | 5. FUNDING NUMBERS                                  |   |
| 6. AUTHOR(S)<br><br>Leloudas, Fragiskos   |  |   |   |   |
| 7. PERFORMING ORGANIZATION NAME(S) AND ADDRESS(ES)<br><br>Naval Postgraduate School<br>Monterey, CA 93943-5000  |  |   |   |   |
| 9. SPONSORING / MONITORING AGENCY NAME(S) AND ADDRESS(ES)   |  |   | 10. SPONSORING / MONITORING<br>AGENCY REPORT NUMBER |   |
| 11. SUPPLEMENTARY NOTES<br>The views expressed in this thesis are those of the author and do not reflect the official policy or position of the Department of Defense or the U.S. Government.   |  |   |   |   |
| 12a. DISTRIBUTION / AVAILABILITY STATEMENT<br><br>Approved for public release; distribution unlimited   |  |   | 12b. DISTRIBUTION CODE                              |   |
| 13. ABSTRACT (maximum 200 words)<br><br>This thesis details the design of Ground Support Equipment (GSE) for the Naval Postgraduate School's Ionospheric Spectroscopy and Atmospheric Chemistry (ISAAC) Ultraviolet Spectrograph. ISAAC is one of the several experiments to be flown on the Advanced Research and Global Observation Satellite (ARGOS) in 1996. The GSE consists of several software programs written in LabVIEW. These programs simulate the timing signals that ISAAC will receive from the satellite bus. In addition, the programs acquire serial data from ISAAC, perform a serial to parallel conversion and display the resulting spectra. The GSE will allow testing of the spectrograph prior to the interface with the satellite bus. Although the complete flight instrument is not yet available for testing, this thesis describes how the GSE-to-ISAAC interface will be made and how it should be operated. Finally, some hardware/software incompatibilities are identified. |  |   |   |   |
| 14. SUBJECT TERMS<br><br>Ionosphere, Temperature Profiles, Electron Density, Ground Support Equipment   |  |   | 15. NUMBER OF PAGES<br>96                           |   |
|   |  |   | 16. PRICE CODE                                      |   |
| 17. SECURITY CLASSIFICATION OF REPORT<br><br>Unclassified   | 18. SECURITY CLASSIFICATION OF THIS PAGE<br><br>Unclassified | 19. SECURITY CLASSIFICATION OF ABSTRACT<br><br>Unclassified | 20. LIMITATION OF ABSTRACT<br><br>UL                |   |





Approved for public release; distribution is unlimited.

**DEVELOPMENT OF GROUND SUPPORT EQUIPMENT FOR THE NPS  
IONOSPHERIC SPECTROSCOPY AND ATMOSPHERIC CHEMISTRY (ISSAC)  
ULTRAVIOLET SPECTROGRAPH**

Fragiskos Leloudas  
Lieutenant JG., Hellenic Navy  
B.S., Hellenic Naval Academy, 1987

Submitted in partial fulfillment  
of the requirements for the degrees of

**MASTER OF SCIENCE IN PHYSICS**

from the

**NAVAL POSTGRADUATE SCHOOL  
June 1995**

Author: \_\_\_\_\_

Fragiskos Leloudas

Approved by: \_\_\_\_\_

David D. Cleary, Thesis Advisor

Suntharalingam Ganapathigam, Thesis Co-Advisor

William B. Colson, Chairman, Department of Physics

Thesis  
L47867  
C.2

## ABSTRACT

This thesis details the design of Ground Support Equipment (GSE) for the Naval Postgraduate School's Ionospheric Spectroscopy and Atmospheric Chemistry (ISAAC) Ultraviolet Spectrograph. ISAAC is one of the several experiments to be flown on the Advanced Research and Global Observation Satellite (ARGOS) in 1996. The GSE consists of several software programs written in LabVIEW. These programs simulate the timing signals that ISAAC will receive from the satellite bus. In addition, the programs acquire serial data from ISAAC, perform a serial to parallel conversion and display the resulting spectra. The GSE will allow testing of the spectrograph prior to the interface with the satellite bus. Although the complete flight instrument is not yet available for testing, this thesis describes how the GSE-to-ISAAC interface will be made and how it should be operated. Finally, some hardware/software incompatibilities are identified.



## TABLE OF CONTENTS

|  |    |
|--|----|
| I. INTRODUCTION .....  | 1  |
| A. THESIS OBJECTIVES .....                                   | 2  |
| B. THESIS OUTLINE .....                                      | 2  |
| II. BACKGROUND-ARGOS SATTELITE-ISAAC SPECTROGRAPH .....      | 3  |
| A. PHYSICS BACKGROUND .....                                  | 3  |
| 1. Review of Atmospheric Temperature Structure .....         | 3  |
| 2. Review of Molecular Spectroscopy .....                    | 5  |
| 3. Measuring Temperatures in the Thermosphere .....          | 10 |
| 4. Photochemistry of the Ionosphere .....                    | 13 |
| B. ARGOS SATELLITE .....                                     | 17 |
| 1. Electric Propulsion Space Experiment (ESEX) .....         | 20 |
| 2. Unconventional Stellar Aspect (USA) .....                 | 20 |
| 3. Space Dust Experiment .....                               | 21 |
| 4. Critical Ionization Velocity (CIV) .....                  | 21 |
| 5. Extreme Ultraviolet Imaging Photometer (EUVIP) .....      | 21 |
| 6. High Temperature Superconductivity Space Experiment ..... | 21 |
| 7. Global Imaging Monitor of the Ionosphere .....            | 22 |
| 8. High Resolution Airglow and Auroral Spectroscopy .....    | 22 |
| C. ISAAC SPECTROGRAPH .....                                  | 24 |
| 1. Ebert-Fastie Spectrograph .....                           | 24 |
| 2. Image Intensifier .....                                   | 26 |
| 3. CCD Photodetector .....                                   | 26 |
| 4. ISAAC Stepper Motor and Dust Cover .....                  | 27 |
| 5. Stepper Motor Driver .....                                | 27 |
| III. BACKGROUND FOR SOFTWARE .....                           | 29 |
| A. LABVIEW 3.1 .....   | 29 |

|   |    |
|---|----|
| 1. The Front Panel .....                                | 29 |
| 2. The Block Diagram .....                              | 31 |
| 3. The Icon/Connector .....                             | 32 |
| B. NB-DIO32F I/O INTERFACE .....                        | 33 |
| C. NB-TIO-10 I/O INTERFACE .....                        | 36 |
| IV. SOFTWARE DESIGN .....                               | 39 |
| A. ISAAC DATA ACQUISITION BOX.....                      | 39 |
| B. ACQUIRE SPECTRA PROGRAM .....                        | 45 |
| 1. Generation of Clocks .....                           | 46 |
| 2. NB-DIO-32F I/O Interface Configuration .....         | 65 |
| 3. Data Acquisition-Transformation Procedure .....      | 67 |
| a. SubVI BUF READ .....                                 | 67 |
| b. Serial-to-parallel Conversion .....                  | 70 |
| C. GSE INTERFACE-FUTURE CONSTRUCTION OF A GSE BOX ..... | 74 |
| V. RESULTS-SUMMARY OF THE GSE .....                     | 79 |
| A. RESULTS .....  | 79 |
| B. SUMMARY OF THE GSE .....                             | 80 |
| C. FUTURE WORK .....                                    | 81 |
| LIST OF REFERENCES .....                                | 83 |
| INITIAL DISTRIBUTION LIST .....                         | 85 |

## ACKNOWLEDGMENT

This thesis and all my work at the Naval Postgraduate School is dedicated in the memory of my mother.

I am thankful to the Hellenic Navy for giving me the opportunity to study at the NPS. I not only gained high level education, but furthermore I found very challenging the fact that I was studying in a language other than my native.

I would like to thank my advisor professor David D. Cleary for his guidance with this thesis. I would also like to thank my co-advisor professor Suntharalingam Gnanalingam for being such a valuable instructor and for helping me refining the text of this thesis.

Once more, I thank my father for his continuous love, guidance and support throughout my life. I wish that I can be half as good as he is. I thank him for everything, for teaching me mathematics, for making me love Greece and the Aegean sea so much, for showing me how to be honest and fair to people.





## I. INTRODUCTION

The atmosphere is very important for the conditions of life on earth and for many physical applications. Therefore, continuous study of the chemical structure and the properties of the atmosphere is absolutely necessary. The atmosphere is mainly composed of  $N_2$ ,  $O_2$ , and argon. In a very small percentage, about 0.1%, carbon dioxide ( $CO_2$ ), ozone ( $O_3$ ), and nitric oxide are present. Despite its small percentage,  $O_3$  is extremely important for life on earth. There is an ozone layer at an altitude of about 30 km above the surface of the earth that absorbs the solar radiation between wavelengths of 2000-3000 Å. This radiation is lethal and if it reached the earth it would not be tolerated by most forms of life. The atmosphere also warms the earth's surface to an average temperature of 300 K by being transparent to the 6000-K solar blackbody radiation. In addition, the atmosphere is of great scientific interest. The upper atmosphere contains free electrons in sufficient numbers to influence the propagation of radio waves. This region, called the ionosphere, behaves like a diffuse mirror in the sky, and plays an important role in communications over very long distances on the earth's surface, and in over-the-horizon radar.

The Ionospheric Spectroscopy and Atmospheric Chemistry (ISAAC) spectrograph was designed by the Naval Postgraduate School (NPS) in order to allow a greater scientific understanding of the upper atmosphere. ISAAC will be one of many experiments on the Advanced Research Global Observation Satellite (ARGOS) which is to be launched in 1996. The ARGOS experiments will enhance our knowledge of the physics of the atmosphere.

The ISAAC spectrograph will measure the intensities of the ultraviolet spectral emissions of several atomic and molecular constituents of the atmosphere. These measurements will give the opportunity to derive temperature profiles of the upper atmosphere and electron density profiles of the atmosphere. The temperature profiles will provide information essential for many military applications. The electron density

profiles will improve satellite communications, long range communications, over-the-horizon radar and navigational solutions.

## **A. THESIS OBJECTIVES**

This thesis develops a Ground Support Equipment (GSE) for the ISAAC spectrograph. The GSE will allow testing of the spectrograph prior to its connection with the satellite bus. The GSE includes a Macintosh Quadra 650 computer, the NB-TIO-10 timing board, the NB-DIO-32F data acquisition board and software programs written in LabVIEW 3.1. The GSE simulates the signals that ISAAC will receive from the satellite and obtains and displays the data from the ISAAC spectrograph. This project also describes how a GSE box, which will interface the GSE to ISAAC, will be constructed.

## **B. THESIS OUTLINE**

This thesis is divided into five chapters. Chapter II provides the physics background for the ionosphere in connection with the objectives of the ISAAC spectrograph. This chapter also includes a brief presentation of the ARGOS satellite and its eight experiments. In addition, Chapter II describes the ISAAC spectrograph. Chapter III details the software package that was used to write the programs and also presents the two GSE boards. Chapter IV discusses the ISAAC data acquisition box and presents the GSE programs. Chapter IV also describes the construction of a GSE interface box that will link the GSE to ISAAC. Finally, Chapter V contains the results of the GSE, presents a summary of the development of the GSE, discusses outstanding problems of the GSE operation and provides recommendations for future work.

## II. BACKGROUND-ARGOS SATELLITE-ISAAC SPECTROGRAPH

This chapter is divided into three sections. The first section contains the essential physics background as a motivation for the ISAAC experiment. The second and the third sections present the ARGOS satellite and the ISAAC spectrograph, respectively.

### A. PHYSICS BACKGROUND

The classification of the atmosphere into different regions according to temperature variations with altitude is given. The atmospheric temperature structure is discussed along with molecular spectroscopy. The temperature of the uppermost region of the atmosphere, the thermosphere, is discussed. Finally, the photochemistry of the ionosphere is detailed.

#### 1. Review Of Atmospheric Temperature Structure

The atmosphere is the gaseous shell that surrounds the earth. The region of interest to this thesis starts at an altitude of 30 km and extends up to several thousand kilometers. This region is important as a satellite environment. The part of the upper atmosphere that is ionized is called the ionosphere and extends from 50 km to 1000 km altitude. The atmosphere is divided into four regions according to the temperature variations at different altitudes. These regions are the troposphere, the stratosphere, the mesosphere and the thermosphere. Figure 1 illustrates the temperature profile in the atmosphere.

The lowest region of the atmosphere is the troposphere where the temperature decreases with altitude at a fairly uniform rate of  $-6.5^{\circ}\text{C/km}$  up to about 15 km. At this altitude is the tropopause and the temperature reaches a minimum of about  $-60^{\circ}\text{C}$ . The next region of the atmosphere is the stratosphere which is 25 km thick at mid-latitudes. The stratosphere is thicker above the poles and thinner above the equator. Near the base of the stratosphere, the solar ultraviolet radiation is absorbed. Therefore, the temperature in the stratosphere increases with increasing altitude.

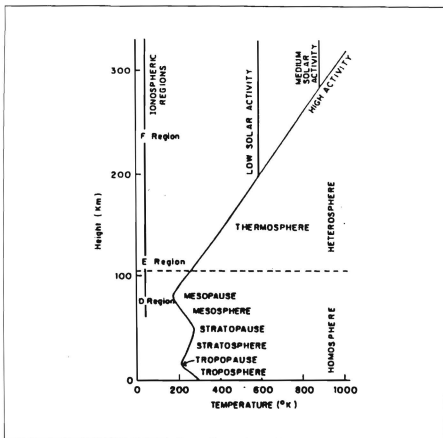


Figure 1. Temperature Profile in the Atmosphere.

This increase stops at the stratopause which is at about 50 km altitude. Above the stratopause is the third region of the atmosphere, the mesosphere. The mesosphere extends up to 80-85 km altitude. Because heat is removed in the mesosphere through radiative cooling, the temperature profile decreases up to the mesopause. The coldest temperatures of the atmosphere (180 K) occur at the mesopause at an altitude of about 85 km.

The region of the atmosphere above the mesopause is the thermosphere. Strong positive temperature gradients occur in the thermosphere. The gradients are caused by the heating of the atmosphere from the absorption of short wavelength solar radiation. The temperature increases up to 300-400 km altitude. Above this altitude the temperature is nearly constant. The high temperatures (1000-1500° K) are primarily caused by the inefficient heat removal processes. The thermosphere absorbs only  $10^{-6}$  of the solar energy supplied to earth. The rest is absorbed by the lower atmosphere and the ground.

One of the priorities of ISAAC is to measure temperature profiles in the thermosphere. These profiles can be determined from the molecular spectra. Below a brief presentation of diatomic molecular spectroscopy is given.

## 2. Review Of Molecular Spectroscopy

Diatomic molecules are important constituents of the atmosphere. The diatomic molecule can be modeled by two spheres of mass  $m_1$  and  $m_2$  separated by a distance  $R$  and bound by an electrostatic attraction. Molecules can remain bound in the ground as well as in excited states. The nuclei in a molecule can move relative to one another. The nuclei can vibrate about the equilibrium separation and in addition, the whole system can rotate about its center of mass. The energy in each of these motions in a molecule is quantized. More energy levels are expected in a molecule than in an atom. The energy of a molecule is made up of three principal parts: electronic, vibrational and rotational. The molecular energy levels are divided into groups which correspond to different electron states of the molecules. For each electronic state there are groups of successive vibrational states of the nuclei. Finally, within each vibrational state there are different rotational states of the molecule.

The rotational motion of a diatomic molecule can be thought of as the rotation of a rigid body about its center of mass. The center of mass lies on the axis connecting the nuclei. The energy of a rotational state is given by

$$E_r = \frac{h^2}{8\pi^2 I} r(r+1) \quad (1)$$

where  $r = 0, 1, 2, \dots$  is the rotational quantum number,  $h$  is Planck's constant and  $I$  is the rotational moment of inertia about the axis of rotation due to the nuclei.  $I$  is given by

$$I = \mu R_0^2 \quad (2)$$

where  $R_0$  is the equilibrium separation of the nuclei and  $\mu$  is the reduced mass of the system. Successive rotational states will be separated in energy by

$$\Delta E_r = \frac{h^2}{4\pi^2 I} r \quad (3)$$

The allowed transitions between rotational states are given by the selection rule  $\Delta r = \pm 1$ .

As mentioned above, the nuclei in the molecule do not maintain a fixed separation but rather they vibrate about the equilibrium separation. This vibrational energy is quantized according to

$$E_u = (u + \frac{1}{2}) h \nu_0 \quad (4)$$

where  $u = 0, 1, 2, \dots$  is the vibrational quantum number and  $\nu_0$  is the classical vibration frequency given by

$$\nu_0 = \left( \frac{1}{2\pi} \right) \sqrt{\frac{C}{\mu}} \quad (5)$$

where  $C$  is the force constant of the molecule.

From Equation 4 it can be seen that there is a zero point energy  $(\frac{1}{2})h\nu_0$  and subsequent vibrational energy levels are equally spaced. Equation 4 is only an approximation since, as the energy increases and the potential energy curves become anharmonic, the levels are not equally spaced but get slightly closer to one another. If the molecule has a permanent electric dipole moment at the equilibrium internuclear separation, it will exhibit vibrational transitions due to oscillations in the dipole moment.

The selection rule for these transitions is  $\Delta u = \pm 1$  so that  $\Delta u = h\nu_0$ . In a vibrational transition the molecule may also change its rotational state. This produces a vibration-rotation spectrum. Figure 2 shows the energy level diagram for vibrational and rotational transitions of a diatomic molecule. These transitions form a band of equally spaced lines. Note that the transitions  $\Delta r=0$ , which would yield photons of the same frequency, are forbidden and hence missing from the spectrum.

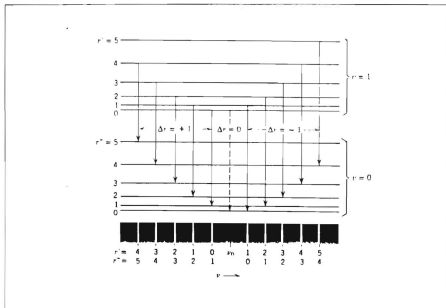


Figure 2. Energy Level Diagram for Vibrational and Rotational States of a Diatomic Molecule. (Eisberg and Resnick, 1985).

In addition to rotational and vibrational states, molecules also have electronic states. Figure 3 shows the molecular energy versus the internuclear separation for two electronic states.



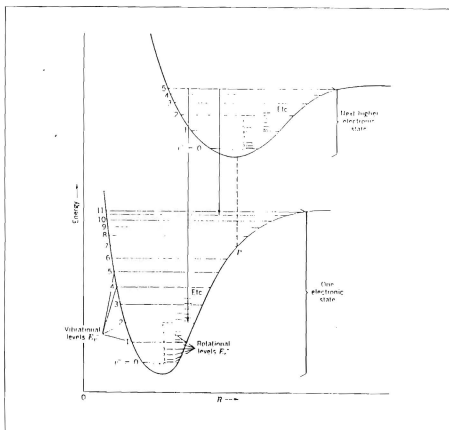


Figure 3. The Molecular Energy versus Internuclear Separation Curves for two Electronic States. (Eisberg and Resnick, 1985).

As discussed above, for each electronic state  $E_e$ , there are many corresponding vibrational states  $E_v$ , and for each vibrational state there are many corresponding rotational states  $E_r$ . The total molecular energy can be written as

$$E = E_e + E_v + E_r \quad (6)$$

and the energy in all three modes may change in an electronic transition so that the total change in energy is given by

$$\Delta E = \Delta E_e + (E'_v - E''_v) + (E'_r - E''_r) \quad (7)$$

where  $\Delta E_e$  is the electronic energy difference. In general many transitions are allowed and a complex spectrum of lines is produced. Figure 4 shows the transitions leading to the formation of an electronic band.

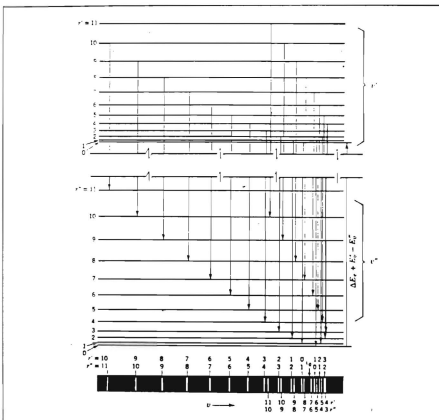


Figure 4. Energy Level diagram and Transitions Leading to the Formation of an Electronic Band. (Eisberg and Resnick, 1985).

### 3. Measuring Temperatures in the Thermosphere

As discussed above one of the priorities of ISAAC is to obtain temperature profiles of the thermosphere. The region of the atmosphere from 110-140 km altitude is very important for the temperature profile since there is a steep gradient in this region. Thermospheric temperature profiles are usually derived by models such as the Mass Spectrometer Incoherent Scatter or MSIS (Hedin, 1987) rather than from direct measurements. Barth and Epavier (1993) presented a method to measure temperatures in the lower thermosphere. Barth and Epavier use the rotational structure of the nitric oxide Gamma bands that are excited in the day airglow. This technique involves comparison of synthetic spectra with observed spectra.

The nitric oxide Gamma bands are produced in the transitions between the ground  $X^2\Pi$  state and the excited  $A^2\Sigma^+$  state. Each individual Gamma band corresponds to transitions between a vibrational level  $u'$  in the excited electronic state  $A^2\Sigma^+$  and a vibrational level  $u''$  in the ground electronic state  $X^2\Pi$ . Each band consists of hundreds of rotational lines in twelve branches. The details of the rotational structure depend on the line strengths of the rotational transitions in absorption and emission and on the population of the rotational levels of the ground state nitric oxide molecules. The latter is temperature dependent.

Barth and Epavier (1993) developed an algorithm to calculate the synthetic spectra of the NO Gamma bands. Figure 5 shows the rotational structure of the (1,1) Gamma band for the temperatures of 280 K and 710 K. This figure clearly shows a temperature dependence on the rotational structure.

Figure 6 shows plots of four spectra observed between the altitudes 110-140 km. The calculated spectra derived from this analysis are overplotted with the experimental data. In all cases the fit is generally good. The temperature data that were derived from rocket spectra by Barth and Epavier have been plotted for comparison with the temperatures calculated by the MSIS. Figure 7 shows the results where the crosses represent the data from the rocket experiments and the solid line is the temperature profile

determined by the MSIS model. The size of each cross indicates the uncertainty in the temperature measurements. Thus, it is possible to infer the thermospheric temperatures using the rotational structure of the (1, 1) Gamma bands of the nitric oxide. ISAAC will enable us to perform such measurements continuously from a spaceborn platform.

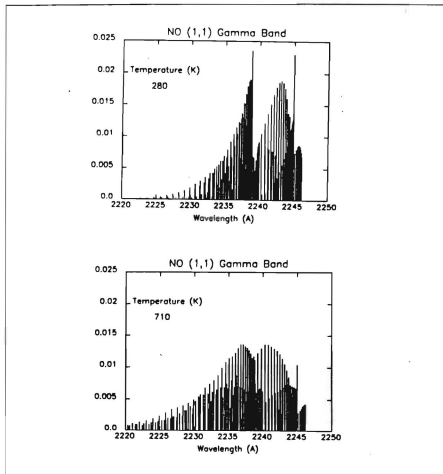


Figure 5. Rotational Structure of the (1,1) NO Gamma Band for 280 K and 710 K. (Barth and Epavier, 1993).

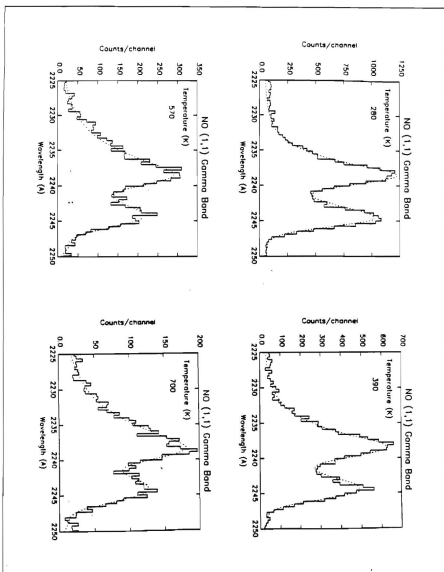


Figure 6. Comparison of synthetic and observed spectra for the  $(1,1)$  NO Gamma Band at four Altitudes: 110 km (280 K), 120 Km (390 K), 130 Km (570 K) and 140 Km (700 K). (Barth and Epavier, 1993).

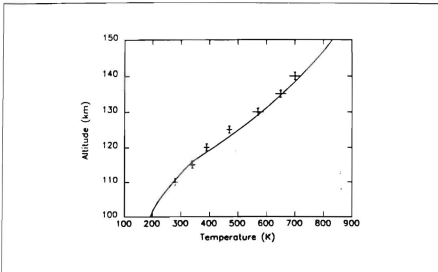


Figure 7. Comparison of Temperatures Determined from the Rocket Observation (Crosses) and the MSIS Model (Solid Line). (Barth and Epavier, 1993).

#### 4. Photochemistry Of The Ionosphere

The ionosphere is the region of the upper atmosphere that is partially ionized. The ionosphere extends from 50 km to 1000 km altitude and reflects radio waves of frequencies up to several MHz. The charged particles are produced in part by the ionization of neutral gases by the solar ultraviolet and x-radiation. The ionosphere is not only composed of charged particles. Neutral particles are also present and in much greater numbers than the ions and electrons. A list of the important gases in the atmosphere and their respective ionization potentials is given in Table 1.

| Gas            | Ionization Potential (eV) |
|----------------|---------------------------|
| N <sub>2</sub> | 15.58                     |
| O <sub>2</sub> | 12.1                      |
| O              | 13.61                     |
| NO             | 9.25                      |
| He             | 24.58                     |
| H              | 13.59                     |

Table 1. Gases of the Atmosphere and their Ionization Potentials.

The variation of electron density with altitude led to the subdivision of the ionosphere into four regions, the D, E, F1 and F2 regions. Figure 8 shows the electron density as a function of altitude. The regions of the ionosphere are the following:

1. The D-region extends from 50 km to 90 km altitude. The electron densities in this region are about  $10^3$ - $10^4$  cm<sup>-3</sup>. The D-region disappears at night due to the absence of the incident radiation. The principal ions in the D-region are the 'water cluster' ion H<sub>3</sub>O<sup>+</sup> - H<sub>2</sub>O, the metal ions Mg<sup>+</sup> and Na<sup>+</sup>, and NO<sup>+</sup>.
2. The E-region extends from 90 km to 140 km altitude. During daytime the maximum electron density is about  $10^5$  cm<sup>-3</sup> at an altitude of about 100 km. The E-layer usually disappears during the night. The dominant ions in the E-region are the O<sub>2</sub><sup>+</sup> and the NO<sup>+</sup>.
3. The F1-region which extends from 140 km to 200 km altitude. It occurs only during daytime and has electron density  $10^5$  cm<sup>-3</sup>. The F1-region is most pronounced during summer and high solar activity levels. The dominant ions in this region are the O<sup>+</sup>, NO<sup>+</sup> and O<sub>2</sub><sup>+</sup>.
4. The F2-region extends above 200 km altitude and has the highest electron densities that occur in the ionosphere. The electron density there is about  $2 \times 10^6$  cm<sup>-3</sup> and is greater during daytime. The important ions in the F2-layer are the O<sup>+</sup> with some N<sup>+</sup>. Above the F2-layer is the topside ionosphere which is highly

ionized and merges into radiation belts at 2000-3000 km altitude. The F1 and the F2-layers form the F-region which is the most important of the ionospheric regions since it is responsible for high frequency wave reflection and Over-the-Horizon Radar.

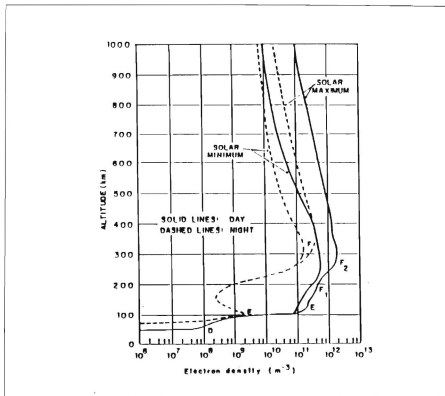


Figure 8. Electron Density as Function of Altitude in the Ionosphere. (Heinz and Olsen, 1994).



As mentioned above, the positive ions  $\text{NO}^+$  and  $\text{O}_2^+$  are the dominants ions in the E and F1-regions while the F2-region is almost exclusively composed of  $\text{O}^+$ . The production of ions is balanced by losses due to chemical reactions and transport out of the region (diffusion). Diffusion is more important at high altitudes while at low altitudes losses are mostly caused by chemical reactions. Each of the ions obeys the Mass Continuity Equation. In one dimension this equation can be written as

$$\frac{\partial n}{\partial t} = P - Ln - \frac{\partial \phi}{\partial z} \quad (8)$$

where  $n$  is the number density of the ion,  $P$  is chemical production,  $L$  is the chemical loss and  $\phi$  is the vertical flux.

There are several models that calculate the density of ions in the ionosphere. One of these is the Photochemical Model of the Ionosphere developed by Cleary (1986). This model allows the determination of the densities of  $\text{NO}^+$ ,  $\text{O}_2^+$ ,  $\text{N}_2^+$ ,  $\text{N}^+$  and  $\text{O}^+$ . This model requires the following inputs:

1. The density profiles of  $\text{N}_2$ ,  $\text{O}_2$  and  $\text{O}$ . These profiles are currently provided by MSIS.
2. The temperature profile of the ionosphere. This is currently provided by MSIS.
3. The solar flux spectrum. The Hinteregger (1974) model currently provides the spectrum.
4. The photoelectron flux. Currently this is provided by a model developed by Anderson and Meier (1982).

Photoelectrons are generated in the following way. When a photon is absorbed by an atom it may ionize it if it has energy higher than the ionization potential of the atom (see Table 1). Then, an ion and an electron are produced. The amount of photon energy in excess of the atoms ionization potential is divided between the ion and the electron. The electron, having less mass, takes most of this excess energy. This energetic electron

is called a photoelectron. For example, consider the photoionization of an O atom. If the photon has energy above 13.61 eV then the following occurs



where  $\text{e}^*$  is a photoelectron.

The ISAAC spectrograph will contribute to the inputs required for the photochemical model of the ionosphere by measuring the density profiles of  $\text{N}_2$ ,  $\text{O}_2$  and O and the temperature profile of the ionosphere. The model can then be constrained to predict the densities of  $\text{NO}^+$  and  $\text{O}_2^+$  which are the dominant ions in the important E and F1-regions. Thus, the second major objective of the ISAAC spectrograph will be to help determine ionospheric densities.

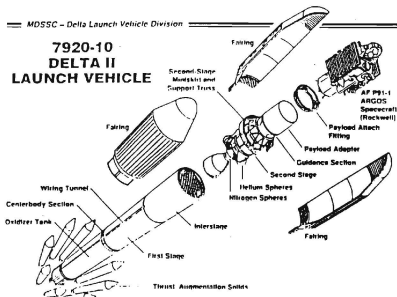
## **B. ARGOS SATELLITE**

The ISAAC spectrograph will fly on the Advanced Research and Global Observation Satellite (ARGOS) which is to be launched in 1996. The satellite weighs 6000 lbs and has a 44 ft span across the solar arrays. ARGOS will be placed in its orbit by a Delta II 7920-10 launch vehicle. The orbit will be at a relatively low altitude (450 nm) and sun-synchronous with a  $98.7^\circ$  inclination. The launch vehicle is shown in Figure 9 and the launch profile is displayed in Figure 10.

ARGOS will have eight experiments onboard. These experiments include several subexperiments and a total of 31 sensors. Figure 11 shows the integrated space vehicle and the payload complement. The eight experiments on ARGOS are the following: ESEX, CIV, GIMI, USA, EUVIP, SPADUS, HTSSE II and HIRAAS. ISAAC is a subexperiment on the HIRAAS experiment. Below a brief presentation of each one of the eight experiments is given.

MDSSC - Delta Launch Vehicle Division

# 7920-10 DELTA II LAUNCH VEHICLE



Rockwell International  
Space Systems Division

Figure 9. 7920-10 Delta II Launch Vehicle.

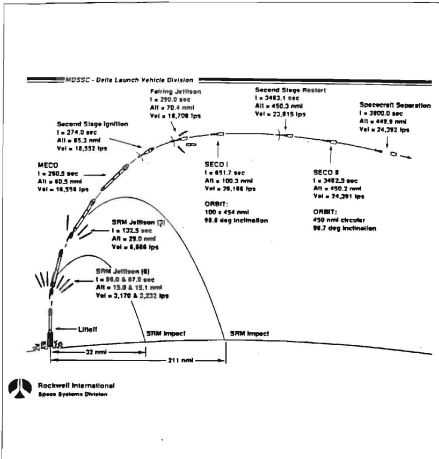


Figure 10. ARGOS P91-1 Launch Ascent Profile.

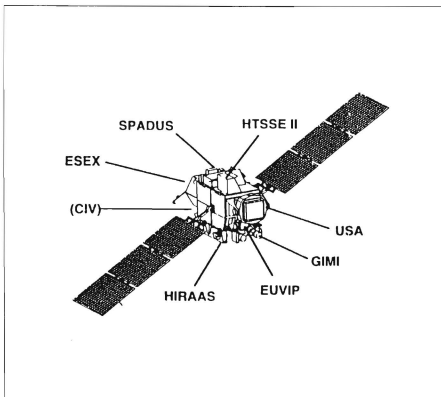


Figure 11. ARGOS Space Vehicle and Payload Configuration.

### 1. Electric Propulsion Space Experiment (ESEX)

ESEX is a 26 kW class ammonia arcjet that gives a specific impulse of 800 seconds (vacuum) at a thrust level of 2 W. This arcjet will demonstrate electric propulsion technology required for low cost access to space. It will operate for ten 15-minute firings while collecting performance data.

### 2. Unconventional Stellar Aspect (USA)

The USA experiment has two counter detectors. These detectors will measure x-rays in the 1-15 KeV range. USA will be used to study astronomical x-rays. The

information obtained will determine whether these x-rays can be used for positional information of autonomous military space systems. Finally, USA will conduct the first x-ray tomography survey of the atmosphere of the earth.

### **3. Space Dust Experiment (SPADUS)**

This experiment will measure the mass, velocity, flux, charge and trajectory of dust particles that are 2-200  $\mu\text{m}$  in size. In addition, SPADUS will measure the radiation environment in the region of 0.2-20 MeV. The collection of the dust particles will be carried out using two parallel grids of 32 polyvinylidene fluoride sensors oriented in the velocity vector direction. The information acquired from the dust particles will provide measurements of the orbital debris at an altitude of 450 nm and will allow spatial mapping of the dust distribution. The radiation measurements will aid to the design of electronics and shielding that will provide resistance to this environment.

### **4. Critical Ionization Velocity (CIV)**

This experiment is a follow-on to a previous CIV experiment and will provide the essential information required to improve our ability to measure rocket and spacecraft plumes. CIV will release xenon and carbon dioxide to observe the ionization processes caused in the upper atmosphere by molecular collisions. Carbon dioxide will be released to study its reaction with the atmosphere. CIV will observe Xenon ion formation, optical signature and spatial distribution.

### **5. Extreme Ultraviolet Imaging Photometer (EUVIP)**

The EUVIP photometer is mounted in the space vehicle with 5° circular field-of-view. EUVIP will measure stellar and atmospheric spectra at three wavelengths: 100Å, 304Å and 834Å. This experiment will study the ionosphere's F1 and F2 regions, the auroral oval and the EUV celestial source.

### **6. High Temperature Superconductivity Space Experiment (HTSSE II)**

This experiment will test the High Temperature Superconductivity (HTS) technology. The HTS technology is digital and will provide ten times more speed than silicon or gallium arsenide technology.

## **7. Global Imaging Monitor of the Ionosphere (GIMI)**

This experiment will observe the airglow and aurora along with HIRAAS and ISAAC. GIMI will obtain ultraviolet images to monitor the electron density and the ionospheric  $O^+$  in the upper atmosphere. The experiment's objectives include:

- observation of NO nightglow through which measurements of atomic nitrogen in the middle atmosphere may be inferred.
- observation of the occultation of bright UV stars by the atmosphere which will demonstrate the remote sensing of the neutral atmosphere ( $O_2$ ,  $N_2$ ) at night.
- wide-field imaging of celestial sources (stars, nebulae and diffuse background) in the 920-1100Å and 1310-1600Å wavelength ranges.

GIMI will obtain data of the ultraviolet emissions in the 750-1050Å and 1310-1600Å wavelength ranges. In particular, the experiment will allow observation of the 834Å  $O^+$  dayglow emission and the 1356Å  $O$  nightglow emission. The sensors required are placed on a two axis gimbal allowing observation of celestial targets and earth ionospheric emissions.

## **8. High Resolution Airglow and Auroral Spectroscopy (HIRAAS)**

HIRAAS includes three UV spectrographs. These spectrographs are the High Resolution Ionospheric Thermospheric Spectrograph (HITS), the Low Resolution Airglow/Aurora Spectrograph (LORAAS) and the ISAAC spectrograph. Figure 12 shows HIRAAS with its three spectrographs.

LORAAS has a fixed passband from 800-1700Å with a 12Å resolution. It is an optical copy of the DMSP special sensor for UV Limb Imaging (SSULI) and it will provide the opportunity for calibration before the first flight of SSULI. HITS gives an 80Å selectable passband in the 500-1500Å range with resolution less than 0.5Å. ISAAC has a spectral range of 1800-3300Å with 2.5Å resolution.

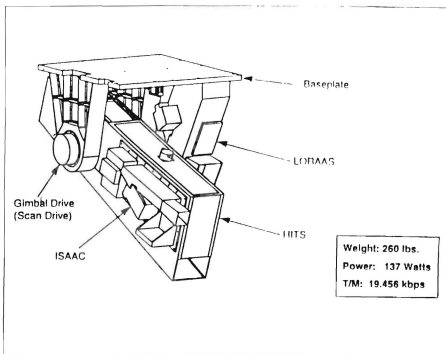


Figure 12. HIIRAAS Assembly.

HIITS and ISAAC are mounted on a scanning platform that will scan the earth's limb by performing a slow downward scan at 90 seconds. This scan will observe tangent altitudes between 0-750 km.

Objectives of the HIIRAAS array of spectrographs are:

- Perform a high spectral resolution study of thermospheric and Ionospheric EUV/FUV/MUV airglow.
- Measure vertical profiles of the major and minor atmospheric constituents to study photochemistry, thermodynamics, and coupling between regions.
- Develop and test a new technique for 3-D ionospheric remote sensing.



- Use high resolution spectroscopy to study radiation transfer in optically thick lines in the earth's atmosphere.
- Measure the distribution of odd nitrogen in the lower thermosphere to help determine densities in the E and F1 regions of the ionosphere.
- Measure temperature profiles of the thermosphere.
- Use high spectral resolution to determine Doppler widths and shifts of precipitating ions in proton auroras.
- Study the effects of the buildup of greenhouse gases on the composition and thermal structure of the upper atmosphere.

### **C. ISAAC SPECTROGRAPH**

ISAAC was designed at the Naval Postgraduate School and fabricated by Research Support Instruments, Inc. It consists of a 1/8-m Ebert-Fastie spectrograph with a moveable reflecting diffraction grating, a 1/8-m off-axis parabolic telescope and an image intensifier connected to a linear CCD photodetector. The diffraction grating may be rotated to one of four positions through a stepper-driver motor. A mechanical dust cover door is located at the entrance of the telescope. The grating stepper motor and the dust cover door can be controlled by the RSI Model 480-229 Stepper motor driver. The latter driver provides an interface between the spacecraft bus and the ISAAC stepper motor and dust cover door.

#### **1. Ebert-Fastie Spectrograph**

ISAAC includes a 1/8-m off-axis parabolic telescope mirror, a 1/8-m Ebert mirror and the diffraction grating which has 3600 grooves/mm. Figure 13 shows the light path in the spectrograph. As the light enters the telescope, it is reflected from the telescope mirror and then is focused at a 75  $\mu$ m wide 2.52 mm long entrance slit. After that light is reflected from the 1/8-m Ebert mirror and is collimated into the reflecting plane-diffraction grating. Light is dispersed from the grating back to the Ebert mirror which focuses light onto an image intensifier.

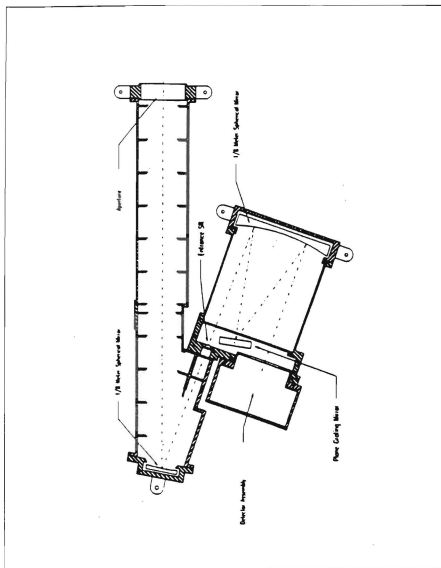


Figure 13. Light Path in the ISAAC Spectrograph.

## **2. Image Intensifier**

The intensifier used is an ITT F4145 Proximity Focused Channel Intensifier Tube with Dual Microchannel Plates. It consists of a quartz input window, a cesium telluride (CsTe) photocathode, two microchannel plates, a phosphor-coated aluminum screen and a fiber optic output window. The intensifier amplifies and converts ultraviolet photons to visible photons at a wavelength near the peak of the CCD photodetector's sensitivity curve.

The UV photons at the exit focal plane of the spectrograph strike the photocathode and produce photoelectrons. These electrons are accelerated to the first microchannel plate. A variable 400-2000 V voltage applied across the first plate provides more acceleration to the incoming photoelectrons. For each electron that enters the first plate, approximately 300 exit. These electrons enter the second microchannel plate where they are again multiplied by 300. Approximately  $10^5$  electrons exit the second plate for each electron that enters the first one. These electrons are accelerated onto a phosphor-coated aluminum screen through an electric field induced by a voltage of about 6000 V applied between the microchannel plate and the aluminum screen. Visible photons are produced as the accelerated electrons strike the screen.

## **3. CCD Photodetector**

The Hamamatsu 53904 Linear Image Sensor is a linear array of 1024 p-n junction photodiodes that offer low dark current and high sensitivity. The 1024 photodiodes are 2.5 mm in height with a 25  $\mu\text{m}$  pitch. They convert the optical energy of incident photons into electrical energy which is stored as a charge in a capacitor. The photodiodes are sensitive to light in the wavelength range 2000-11000Å. The peak sensitivity is at 6000Å. For this reason the image intensifier has a phosphor screen that converts ultraviolet light to visible light.

The charge stored in each photodiode is successively transferred by a shift register. This shift register uses three clock signals that are generated by the C4350 Driver/Amplifier Circuit. This circuit provides the timing signals to drive the MOS

sensor and also provides a charge amplifier used to read out the video data, Sample-and-Hold and End-of-Scan. A 15-pin connector provides the interface for these signals (for the pinouts of this connector see MacQuarrie, 1994). The Video-Data is the integrated, low noise video signal of the MOS Image Sensor. A Sample-and-Hold is used for A/D conversion while the End-of-Scan line signals the end-of-signal from the MOS shift register. This thesis develops a GSE that will test the ISAAC spectrograph. The GSE, among other functions, will receive the video data from the ISAAC detector and displays them on a graphic screen.

#### **4. ISAAC Stepper Motor and Dust Cover**

The stepper motor allows selection of one of the following four wavelength ranges, determined by MacQuarrie (1994), for the diffraction grating

- Position 1      1817-2290 Å
- Position 2      2203-2656 Å
- Position 3      2609-3026 Å
- Position 4      2898-3290 Å

The initial position of the grating is identified by a fiducial signal. A cable that terminates in a 15-pin female I/O connector provides an interface between the motor and the motor controller.

The mechanical dust cover door is located near the entrance to the telescope. The spring-loaded door is controlled by a solenoid and protects the optics of ISAAC during launch and during the release of gases by ARGOS. A 9-pin I/O connector provides the interface between the door and its controls.

#### **5. Stepper Motor Driver**

The Stepper Motor Driver provides an interface between the spacecraft bus and the ISAAC stepper motor and dust cover door. The RSI Model 480-229 Stepper Motor Driver has three interfaces J1, J2, and J3. J1 is a male 32-pin connector that controls the

door position and stepper motor. J2 is a male 15-pin connector that links to the 15-pin output from the stepper motor of ISAAC while J3 is a male 9-pin connector that provides the link to the dust cover door of ISAAC. For the pinouts of J1, J2, and J3 along with more technical data for the ISAAC spectrograph see Macquarrie (1994).

### **III. BACKGROUND FOR SOFTWARE**

This chapter describes the software package and the data acquisition boards that are used in the ISAAC GSE. The GSE software will be presented in the next chapter.

The program was written in LabVIEW 3.1, published by National Instruments. The two data acquisition boards used are the NB-TIO-10 and the NB-DIO-32F also by National instruments. These boards can be used for data acquisition and interface with electronic components. In the next sections LabVIEW 3.1 and the boards will be described.

#### **A. LABVIEW 3.1**

Labview is a program development application using a graphical programming language called G to create programs in block diagram form. LabVIEW includes libraries of functions and development tools designed for data acquisition and instrument control. LabVIEW programs are called virtual instruments ( VIs ) and they are analogous to functions and subroutines from other conventional languages. VIs are hierarchical. They can be used as programs or as subprograms ( subVIs ) within other programs. Each VI has three main parts: the front panel, the block diagram and the icon/connector. Each VI has two separate but related windows. The panel window contains the front panel of the VI and the icon/connector. The diagram window contains the block diagram.

##### **1. The Front Panel**

The front panel is the user interface of a VI and it simulates the panel of a physical instrument. It contains two types of objects: controls and indicators. Controls and indicators are the interactive input and output terminals of a VI. Controls represent the instrument's input devices and provide data to the block diagram of a VI. The indicators simulate instrument output devices that display data acquired or generated by the block diagram of a VI.

Controls and indicators can have several forms, i.e. numeric, Boolean, string and table, array and cluster, etc. For instance the numeric form is used for entering and displaying numeric quantities while the Boolean form is used for entering and displaying true/false quantities.

As an example, Figure 14 illustrates the panel window of a VI that performs the Boolean NAND operation between two Boolean numbers. Two Boolean controls, control A and control B, and one indicator,  $Q=A \text{ NAND } B$ , are used. These controls and indicator will be 'wired' together in the block diagram as explained below.

Generally, through the front panel the user has the ability to enter inputs, observe outputs, and control a program, i.e. run and stop it.

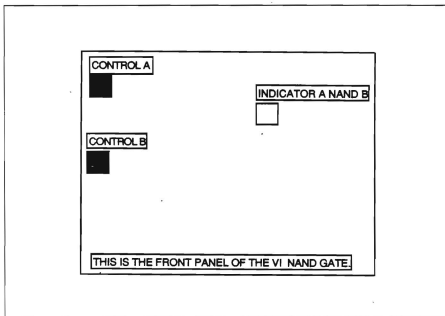


Figure 14. The Front Panel of the NAND GATE VI.

## 2. The Block Diagram

The block diagram is the source code of the VI represented in a pictorial format. The language used to construct the block diagram is G. The block diagram is programmed by 'wiring' together objects that send or receive data. Wires are paths through which data pass between source and destination terminals. The flow of execution of a VI is determined by the manner in which objects are 'wired' together on the block diagram. Figure 15 displays the block diagram of the sample VI described above. Pictured there are the block diagram representations of the two controls and one indicator along with the VI that performs the Boolean NAND operation. The NAND has two input terminals and one output. Notice that the block diagram representation of the two controls are 'wired' to the input terminal of the NAND VI and that the output terminal is connected to the block diagram representation of the indicator. Now that the block diagram is built, the program is ready to run. Both the panel and the diagram windows contain a palette of command buttons and status indicators to control the VI. In Figure 14 the two controls were in the same 'on' state so that the NAND operation puts the indicator in the 'off' state. Every other state combination of the controls would result in the output 'on' state.

The block diagram can also contain objects that are used to control the program flow. These objects are called structures. One of the LabView structures that control program flow is the *Sequence Structure*. It consists of one or more frames that execute sequentially. The *Sequence Structure* is used when one has parts of a program that must be executed in a specific order. The part of the diagram required to be executed first is put in frame 0 of the *Sequence Structure*, the portion to be executed second in frame 1, and so on. Data can be passed to successive sequence structure frames using a sequence local. Data cannot be passed to a preceding frame. The data leave the structure only when the last frame is executed. A *For Loop* is another structure that may also be used. It has two terminals: the count terminal, N, and the iteration terminal, i. The *For Loop* executes its subdiagram *count* times, where the count equals the value contained in the



count terminal. The count can be set explicitly by 'wiring' a value to the count terminal. The count may also be set implicitly with autoindexing. When an array of any dimension is wired from an external node to an input tunnel of the loop border, the value of count is automatically set to the number of elements in the array. Components of that array enter the loop one at a time starting with the first component. Data can be obtained only after the diagram within the *For Loop* is executed for the last time. The iteration terminal contains the current number of completed iterations: 0 during the first one, 1 during the second and so on up to N-1. Finally, there are two more LabVIEW structures; the *While Loop* and the *Case Structure*. These structures are not used in this work but they are analogous to the While and Case statements of other languages.

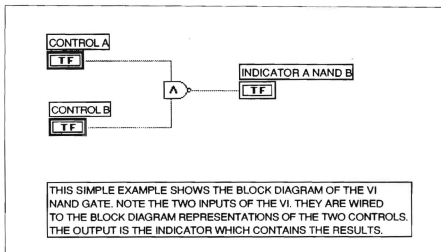


Figure 15. The Block Diagram of the NAND GATE VI.

### 3. The Icon/Connector

In LabVIEW a VI can be used as a subVI. A subVI is analogous to a subroutine in other programming languages. When this subVI is called, the controls receive data and

the indicators return data to the 'calling' VI. The connector is a set of terminals corresponding to specific controls and indicators of the subVI. This means that data can be received at the connector's input terminals or sent out at the respective output terminals. LabVIEW gives the ability to select from a list of connector styles. The icon is simply a representation of the VI in the block diagram of another VI. In other words the icon represents the call to of a particular VI. In Figure 16 the icon and the connector for the sample VI is shown. The two controls are connected to the two left terminals of the connector while the indicator is connected to the right one. Should this VI, NAND GATE, be used as a subVI, the two controls would receive and the indicator would return data.

For more information about LabVIEW and the methods used the reader may refer to the *LabVIEW Tutorial for Macintosh, 1994* and to the *LabVIEW User Manual for Macintosh, 1994*.

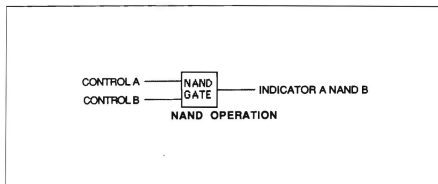


Figure 16. The Icon/Connector of the NAND GATE VI.

#### **B. NB-DIO-32F I/O INTERFACE**

The NB-DIO-32F is a high speed 32-bit parallel digital I/O interface board for Macintosh computer and is supported by the National Instruments LabVIEW software

systems. Specifically, the Labdriver VI library for Labview includes VIs that support the board.

The 50-pin assignment for the NB-DIO-32F digital connector is shown in Table 2. The connector has 32 digital lines, 2 request lines, 2 acknowledge lines, 3 extra digital inputs and 3 extra digital outputs. The 32 lines of digital I/O of the NB-DIO-32F are further divided into four 8-bit ports: Port A, Port B, Port C and Port D. These four ports are grouped into two groups. Ports A and B comprise group 1 while ports C and D form group 2. These groups can operate in handshaking mode; that is, an input port latches the data at the input when a handshake signal is received and generates a handshake pulse when an output port is written to by the computer. The request and acknowledge lines of groups 1 and 2 are REQ 1 and ACK 1 and REQ 2 and ACK 2, respectively.

This board will be used to acquire data from the ISAAC detector. Recall that these data are transferred in a serial format on a single wire. The data are acquired by the NB-DIO-32F board using line 0 of port A, DIOA0 ( pin 37 ). The input handshaking request line for group 1, REQ 1 ( pin 33 ), is given a gated clock of 200 KHz.

As will be explained below, the NB-DIO-32F is configured for handshaking so that data is acquire when the signal applied in REQ 1 shows a rising edge. The clock frequency of 200 KHz was generated by the NB-TIO-10 which will be presented in the following section.

The main purpose of the GSE is to acquire serial data from the ISAAC detector through the NB-DIO-32F board. Once the data are acquired, a serial-to-parallel conversion is performed. In particular, each group of 12 bits acquired serially forms a number. This number represents the intensity received from one photodiode of the ISAAC detector. There are a total of 12288 bits that are converted to form 1024 12-bit numbers. These numbers represent a single spectrum from ISAAC. Once the spectrum is acquired it is displayed on a graphic screen.

|    |       |    |       |
|----|-------|----|-------|
| 1  | DIOD1 | 2  | DIOD4 |
| 3  | DIOD3 | 4  | DIOD0 |
| 5  | DIOD6 | 6  | DIOD7 |
| 7  | DIOD2 | 8  | DIOD5 |
| 9  | DIOC5 | 10 | DIOC7 |
| 11 | DIOC3 | 12 | DIOC1 |
| 13 | DIOC2 | 14 | DIOC0 |
| 15 | DIOC6 | 16 | DIOC4 |
| 17 | GND   | 18 | ACK2  |
| 19 | GND   | 20 | IN2   |
| 21 | GND   | 22 | OUT2  |
| 23 | GND   | 24 | REQ2  |
| 25 | IN3   | 26 | OUT3  |
| 27 | ACK1  | 28 | GND   |
| 29 | IN1   | 30 | GND   |
| 31 | OUT1  | 32 | GND   |
| 33 | REQ1  | 34 | GND   |
| 35 | DIOA4 | 36 | DIOA6 |
| 37 | DIOA0 | 38 | DIOA2 |
| 39 | DIOA1 | 40 | DIOA3 |
| 41 | DIOA7 | 42 | DIOA5 |
| 43 | DIOB5 | 44 | DIOB2 |
| 45 | DIOB7 | 46 | DIOB6 |
| 47 | DIOB0 | 48 | DIOB3 |
| 49 | DIOB4 | 50 | DIOB1 |

Table 2. Pin Assignments for the NB-DIO-32F Board.

### C. NB-TIO-10 I/O INTERFACE

The NB-TIO-10 is a timing and digital I/O interface for Macintosh computers. It uses two Am 9513A STC chips for the timing interface. This board can perform a wide range of timing and digital operations. For the purpose of this thesis it was used to generate several timing signals. The 50 pin connector assignment for the NB-TIO-10 is shown in Table 3.

There are 16 digital lines and 30 connections for timing I/O signals. The 16 digital lines are further divided into two 8-bit ports: Port A and Port B. The 30 timing signals include the GATE, SOURCE and OUT signals for the Am9513A counters 1 through 10 with the exception of counters 5 and 10 which do not have a SOURCE signal. FOUT 1 and FOUT 2, pins 29 and 30 respectively, are the frequency outputs of the two Am 9513A devices. As mentioned above each counter has three pinouts: SOURCE, GATE and OUT. The SOURCE and GATE signals can be directly applied to the counters from the I/O connector so that the counters may be programmed for several tasks. When a counter is configured for square wave generation, several parameters, like the duration of the positive and negative pulse of the wave, can be specified.

The 'count' of a given counter increments with each period of a selected timebase. A signal applied at the SOURCE input can be used as the timebase of any of the counter/timers and by the frequency division output FOUT. Furthermore, the Am9513A generates five internal timebase clocks, from the clock signal supplied by the NB-TIO-10, which may be used as counting sources.

The GATE input may be used to gate counting operations. When a counter is configured for no gating, the counter starts at the first, rising or falling edge (depending on the configuration) of the source/timebase. Once one of the gating modes is enabled, the GATE signal takes effect at the next source/timebase edge and can be used to start or stop counter operation.

|    |          |    |          |
|----|----------|----|----------|
| 1  | SOURCE 1 | 2  | GATE 1   |
| 3  | OUT 1    | 4  | SOURCE 2 |
| 5  | GATE 2   | 6  | OUT 2    |
| 7  | SOURCE 3 | 8  | GATE 3   |
| 9  | OUT 3    | 10 | SOURCE 4 |
| 11 | GATE 4   | 12 | OUT 4    |
| 13 | GATE 5   | 14 | OUT 5    |
| 15 | SOURCE 6 | 16 | GATE 6   |
| 17 | OUT 6    | 18 | SOURCE 7 |
| 19 | GATE 7   | 20 | OUT 7    |
| 21 | SOURCE 8 | 22 | GATE 8   |
| 23 | OUT 8    | 24 | SOURCE 9 |
| 25 | GATE 9   | 26 | OUT 9    |
| 27 | GATE 10  | 28 | OUT 10   |
| 29 | FOUT 1   | 30 | FOUT 2   |
| 31 | EXTIRQ 1 | 32 | EXTIRQ 2 |
| 33 | GND      | 34 | +5V      |
| 35 | A0       | 36 | A1       |
| 37 | A2       | 38 | A3       |
| 39 | A4       | 40 | A5       |
| 41 | A6       | 42 | A7       |
| 43 | B0       | 44 | B1       |
| 45 | B2       | 46 | B3       |
| 47 | B4       | 48 | B5       |
| 49 | B6       | 50 | B7       |

Table 3. Pin Assignment for the NB-TIO-10 Board.

The program of this thesis makes extensive use of the counters of the NB-TIO-10. As will be explained in the following chapter, seven signals are generated for the purpose of obtaining four synchronized signals. The data acquisition box of the ISAAC spectrograph and the GSE communicate with these signals.

## IV. SOFTWARE DESIGN

This chapter details the ISAAC data acquisition box and presents the GSE program, *ACQUIRE SPECTRA*. With the use of this program, the ISAAC data acquisition box and the NB-DIO-32F - NB-TIO-10 boards exchange information. The combination of the Macintosh computer, the NB-DIO-32F, and the NB-TIO-10 boards for the rest of this document will be referred to as the GSE. This chapter also describes how a test interface was built. Finally, this chapter explains how the GSE interface box will be constructed in the future. This box will connect the ISAAC data acquisition box and the GSE interface.

### A. ISAAC DATA ACQUISITION BOX

Figure 17 shows a schematic representation of the ISAAC data acquisition box. This box has five connectors: J301, J302, J303, J310, J311. J301 is a 50-pin connector to the ARGOS Central Electronic (CE) Box. The pinouts for this connector are shown in Table 4. J302 is a 15-pin connector that provides power to the ISAAC detector circuit and provides a connector to the thermal sensors on ISAAC. The pinouts for this connector are shown in Table 5. J303 is a 15-pin connector that provides timing signals to the ISAAC detector circuit. The pinouts for this connector are shown in Table 6. J310 is a 37-pin connector to the motor controller. The pinouts for this connector are shown in Table 7. J311 is a 9-pin connector to the high voltage power supply. The pinouts for this connector are shown in Table 8. Figure 17 shows a schematic presentation of how the five connectors interface the ISAAC data acquisition box, the ISAAC spectrograph, the ARGOS CE box, the stepper motor controller and the voltage supply. This figure also shows the GSE interface which connects to J301 in lieu of the ARGOS CE box. As explained below, the GSE interface serves as a simulation of the ARGOS CE box connector.

The ISAAC data acquisition box receives the analog data from the ISAAC detector board. Recall that ISAAC has a 1024 photodiode array detector. The analog



data contain the intensity detected by these photodiodes. The data acquisition box performs an analog-to-digital conversion. The digital data are transmitted in a serial format on the line IVID-DATA (see Table 4). These data are transmitted at a rate of 200 KHz. A single timing pulse, IVID-STB determines the beginning of each 1024\*12 bit word frame. During one period of IVID-STB 12288 bits are passed to the ARGOS CE box from the ISAAC data acquisition box.

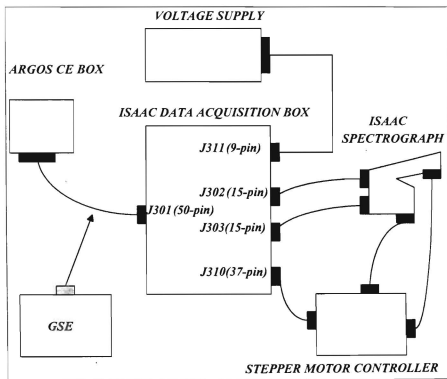


Figure 17. Schematic Diagram showing the Connections between the ISAAC Data Acquisition Box, the ISAAC Spectrograph, the ARGOS CE Box, the Power Supply and the Stepper Motor Controller.

|    |                    |    |                     |
|----|--------------------|----|---------------------|
| 1  |                    | 26 | ICTL-STB+(INPUT)    |
| 2  |                    | 27 | ICTL-STB-(INPUT)    |
| 3  | IGMTR-PWR(INPUT)   | 28 | ITLM-DATA+(OUTPUT)  |
| 4  | IGMTR-RET(INPUT)   | 29 | ITLM-DATA-(OUTPUT)  |
| 5  | IHVPS-PWR(INPUT)   | 30 | IRESET-STB+(INPUT)  |
| 6  | IHVPS-RET(INPUT)   | 31 | IRESET-STB-(INPUT)  |
| 7  | IDET-PWR(INPUT)    | 32 | IVID-DATA+(OUTPUT)  |
| 8  |                    | 33 | IVID-DATA-(OUTPUT)  |
| 9  | ICTL-DATA+(INPUT)  | 34 |                     |
| 10 | ICTL-DATA-(INPUT)  | 35 |                     |
| 11 | ITLM-STB+(OUTPUT)  | 36 | IGMTR-PWR(INPUT)    |
| 12 | ITLM-STB-(OUTPUT)  | 37 | IGMTR-RET(INPUT)    |
| 13 |                    | 38 | IHVPS-PWR(INPUT)    |
| 14 | IVID-START+(INPUT) | 39 | IHVPS-RET(INPUT)    |
| 15 | IVID-START-(INPUT) | 40 | IDET-PWR(INPUT)     |
| 16 | IVID-STB+(INPUT)   | 41 | IDET-PWR-RET(INPUT) |
| 17 | IVID-STB-(INPUT)   | 42 | PULSE-WIDTH+(INPUT) |
| 18 |                    | 43 | PULSE-WIDTH-(INPUT) |
| 19 |                    | 44 | ITLM-CLK+(OUTPUT)   |
| 20 | IGMTR-PWR(INPUT)   | 45 | ITLM-CLK-(OUTPUT)   |
| 21 | IGMTR-RET(INPUT)   | 46 | IVID-EOS+(OUTPUT)   |
| 22 | IHVPS-PWR(INPUT)   | 47 | IVID-EOS-(OUTPUT)   |
| 23 | IHVPS-RET(INPUT)   | 48 | GND(OUTPUT)         |
| 24 | IDET-PWR(INPUT)    | 49 | IVID-CLK+(INPUT)    |
| 25 |                    | 50 | IVID-CLK-(INPUT)    |

Table 4. Pin Assignment of the J301 Connector of the ISAAC Data Acquisition Box.

|   |               |  |    |              |
|---|---------------|--|----|--------------|
| 1 | THERM-REF     |  | 9  | AGND         |
| 2 | THERM-REF-RET |  | 10 | STR/EOS-EN   |
| 3 | +15V-DET/DAQ  |  | 11 | DET-TEMP     |
| 4 | -15V-DET/DAQ  |  | 12 | SPECTRO-TEMP |
| 5 | +5V-DET/DAQ   |  | 13 | GND          |
| 6 | TELESCP-TEMP  |  | 14 | DET-START    |
| 7 |               |  | 15 |              |
| 8 | EOS-DET       |  |    |              |

Table 5. Pin Assignment of the J302 Connector of the ISAAC Data Acquisition Box.

|   |          |  |    |          |
|---|----------|--|----|----------|
| 1 | PHASE-1+ |  | 9  | GND      |
| 2 | PHASE-1- |  | 10 | PHASE-1+ |
| 3 | GND      |  | 11 | PHASE-1- |
| 4 | PHASE-2+ |  | 12 | GND      |
| 5 | PHASE-2- |  | 13 | PHASE-2+ |
| 6 | GND      |  | 14 | PHASE-2- |
| 7 | VIDEO-   |  | 15 | GND      |
| 8 | VIDEO+   |  |    |          |

Table 6. Pin Assignment of the J303 Connector of the ISAAC Data Acquisition Box.

|    |              |    |             |
|----|--------------|----|-------------|
| 1  | HVPS+5V      | 20 | MTR/HV-GND  |
| 2  | HVPS+5V      | 21 | MTR/HV-GND  |
| 3  | HVPS+5V      | 22 | MTR/HV-GND  |
| 4  | HVPS+5V      | 23 | MTR/HV-GND  |
| 5  | STEP-REPEAT  | 24 | CHASSIS-COM |
| 6  | STEP-INPUT   | 25 | GMTR-PWR    |
| 7  | MTR-CURR-MON | 26 | IGMTR-RET   |
| 8  | FIDUCIAL     | 27 |             |
| 9  |              | 28 |             |
| 10 |              | 29 | PRI-PWR     |
| 11 | IDOOR-RET    | 30 | SEC-PWR     |
| 12 | MICRO-Y-NC   | 31 | NORM-PWR    |
| 13 | IDOOR-DRV    | 32 | 3X-PWR      |
| 14 | MICRO-Y-NO   | 33 | RUN-PWR     |
| 15 | MICRO-Y-COM  | 34 | HOLD-PWR    |
| 16 | MICRO-X-NO   | 35 |             |
| 17 | MICRO-X-COM  | 36 |             |
| 18 | MICRO-X-NC   | 37 |             |
| 19 | FIDUCIAL     |    |             |

Table 7. Pin Assignment of the J310 Connector of the ISAAC Data Acquisition Box.

|   |             |  |   |               |
|---|-------------|--|---|---------------|
| 1 | MTR/HV-GND  |  | 6 | HV-MCPIN-MON  |
| 2 | MTR/HV-GND  |  | 7 | HV-MCPOUT-MON |
| 3 | HVPS+5V     |  | 8 | HV-CTRL       |
| 4 | HVPS+5V     |  | 9 | HV-CTRL       |
| 5 | HV-CATH-MON |  |   |               |

Table 8. Pin Assignment of the J311 Connector of the ISAAC Data Acquisition Box.

In order for the data acquisition box to correctly synchronize the transmission of the data, it needs several timing signals from the ARGOS CE box. These signals are:

1. IVID-START. This is a positive pulse sent by the ARGOS CE box once per second that initiates transmission.
2. IVID-STB. This is a negative pulse sent by the ARGOS CE box for every ISAAC spectrum, 16 per second.
3. IVID-CLK. This is a 200 KHz clock corresponding to the serial data output rate. This signal is sent by the ARGOS CE box and is the master clock controlling the whole operation.

The timing relationship between these three clocks is shown in Figure 18.

This project develops a GSE to simulate the ARGOS CE box. The GSE includes a software program that generates the timing signals on the NB-TIO-10 board, acquires the data on the NB-DIO-32F board with handshaking and performs a serial-to-parallel conversion. The interface of the NB-TIO-10 and the NB-DIO-32F boards simulates the CE box connector.

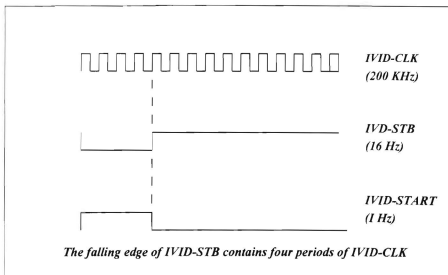


Figure 18. Timing Diagram for IVID-CLK, IVID-STB and IVID-START.

## B. ACQUIRE SPECTRA PROGRAM

As mentioned in Chapter III, the *ACQUIRE SPECTRA* program was written using LabVIEW 3.1 by National Instruments. This program is comprised of five frames of a sequence structure that are executed one after the other in numerical order. In order to generate the three timing signals described above, the program configures four additional signals for internal use. One is the handshake signal for the NB-DIO-32 and the rest help in the generation of the others. These clocks, along with all the other important details of the program are discussed below. The program also configures port A of the NB-DIO-32F board as an input port. This port will receive the signal IVID-DATA from the ISAAC data acquisition box. Since the data are in a serial format, IVID-DATA is connected to the least significant bit of this port, pin DIOA0. Finally, the program strips out the 12288 serial bits and forms 1024-bit words.

## 1. Generation Of Clocks

This subsection describes frames 1, 2 and 3 of the *ACQUIRE SPECTRA* block diagram where the timing signals are generated. These frames are shown respectively in Figures 19, 20 and 21. A summary of these signals is given in Table 9.

Most of these signals are generated by the NB-TIO-10 board in the subVI *TIO CLOCK* which is found in frame 1 of the *ACQUIRE SPECTRA* block diagram. In order to synchronize the timing between ISAAC data acquisition operation and the GSE, a special gating technique is used in frames 2 and 3 as described below.

| SIGNAL           | SOURCE         | GATE      | DESCRIPTION  |
|------------------|----------------|-----------|--|
| IVID-TIM         | Internal(1MHz) | None      | 1 MHz square wave that serves as the master clock  |
| IVID-CLK         | IVID-TIM       | None      | 200 KHz square wave used by the ISAAC data acquisition box   |
| IVID-STB         | IVID-CLK       | Line A0   | 16 Hz square wave used by the ISAAC data acquisition box   |
| IVID-MASK        | IVID-CLK       | Line A0   | 16 Hz square wave used as the timebase of IVID-GATE  |
| IVID-GATE        | IVID-MASK      | None      | Pulse that is used as the gate of IVID-REQ   |
| IVID-REQ         | IVID-TIM       | IVID-GATE | 200 KHz square wave that is the handshaking signal of the NB-DIO-32F board   |
| IVID-START(TEST) | IVID-CLK       | Line A0   | 1 Hz signal that is used by the ISAAC data acquisition box. Since this signal is not required to operate for the purpose of the GSE, it is transformed as IVID-TEST to test the data acquisition |

Table 9. Summary of the Signals Generated by the *ACQUIRE SPECTRA* Program.

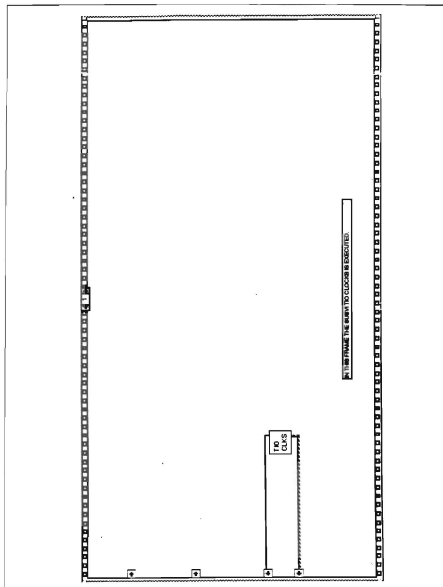


Figure 19. Frame 1 of the *ACQUIRE SPECTRA* Program.



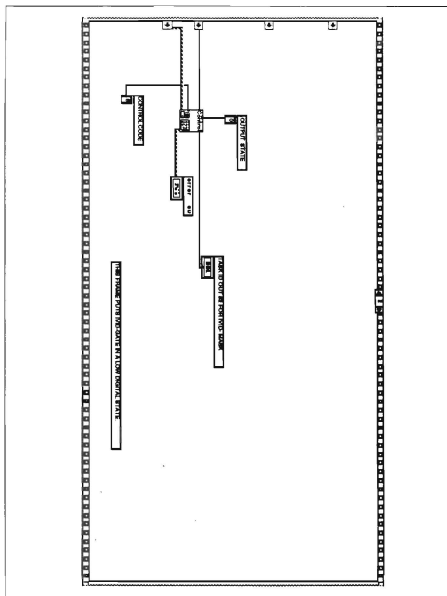


Figure 20. Frame 2 of the *ACQUIRE SPECTRA* Program.

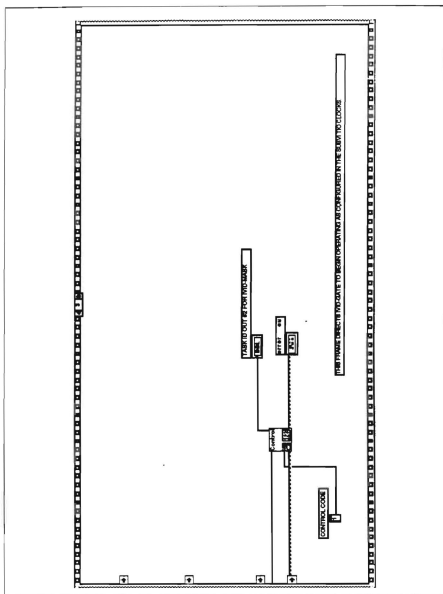


Figure 21. Frame 3 of the *ACQUIRE SPECTRA* Program.

The subVI *TIO CLOCKS* consists of a sequence structure of nine frames. Frame 0 sets line 0 of port A(A0) of the NB-TIO-10 to a digital low state. This line is the gate of IVID-STB, IVID-MASK and IVID-START(TEST). Frame 0 of *TIO CLOCKS* block diagram is shown in Figure 22.

The signal IVID-TIM is generated in frame 1 of *TIO CLOCKS* block diagram which is shown in Figure 23. This signal has a frequency of 1MHz and is generated on the FOUT 1 counter. The signal IVID-CLK has a frequency of 200 KHz and is generated in frame 2 the of *TIO CLOCKS* block diagram which is shown in Figure 24. IVID-CLK is generated on counter FOUT 2 and uses IVID-TIM for its timebase. IVID-CLK is one of the signals used by the ISAAC data acquisition box. The signal IVID-STB is generated in frame 3 of *TIO CLOCKS* block diagram which is shown in Figure 25. IVID-STB is generated on Counter 2. It has IVID-CLK for timebase and line A0 for gate with high level gating mode. The gating mode implies that the counter counts when the gate is high but not when it is low. IVID-STB is one of the signals used by the ISAAC data acquisition box.

Recall that the signal IVID-DATA carries the data from the ISAAC data acquisition box to the ARGOS CE box. The data transmission starts on the thirty-first rising edge of IVID-CLK after IVID-STB shows a leading edge. The 12288 bits of information are followed by a short pause which is followed by 12288 more bits, and so on. The form of IVID-DATA, in connection with the IVID-CLK, is shown in Figure 26. The boxes represent either digital low or high states.

Since data are obtained through handshaking from the NB-DIO-32F, a signal applied at the REQ 1 of this board is required. This signal will control the data acquisition rate. This signal, the IVID-REQ, has a frequency of 200 KHz and it is synchronized with IVID-DATA. Two other signals, the IVID-MASK and IVID-GATE, are used to generate IVID-REQ.

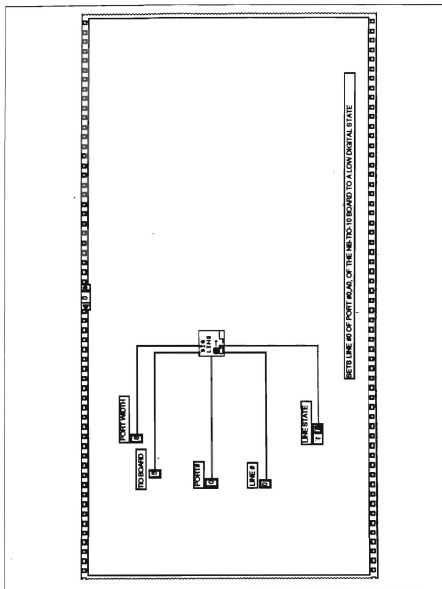


Figure 22. Frame 0 of the SubVI *TIO CLOCKS*.



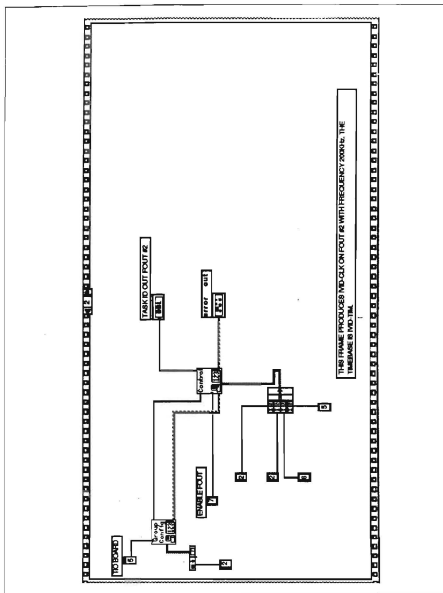


Figure 24. Frame 2 of the SubV1 *TIO* CLOCKS.



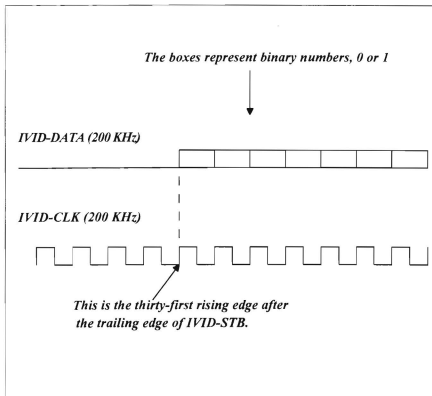


Figure 26. Timing Diagram for IVID-CLK and IVID-DATA.



The 16 Hz clock IVID-MASK is generated in frame 4 of the *TIO CLOCKS* block diagram which is shown in Figure 27. IVID-MASK is generated on Counter 3. It uses IVID-CLK for its timebase and line A0 as a gate with high level gating mode. IVID-MASK is low for 30 timebase periods and high for 12470 periods. The signal IVID-GATE is generated in frame 5 of the *TIO CLOCKS* block diagram which is shown in Figure 28. IVID-GATE is generated on Counter 4 and uses IVID-MASK for its timebase. IVID-GATE is configured for pulse mode with no gating. This pulse is the gate of IVID-REQ. In order to properly synchronize data acquisition, IVID-REQ must start pulsing at the thirty-first rising edge of IVID-CLK after IVID-STB shows leading edge. In order to initiate data acquisition, the counter for IVID-GATE is instructed to count four leading edges from IVID-MASK. At the fourth leading edge it goes high. This enables IVID-REQ which in turn instructs the NB-DIO-32F board to begin acquiring the data at the first data bit transmitted by the ISAAC data acquisition box. In order to give the computer sufficient time to configure all these counters, IVID-GATE is not set to operate until frames 2 and 3 of the *ACQUIRED SPECTRA* diagram are executed. These frames were shown in Figures 20 and 21 respectively. In frame 2 IVID-GATE is set to an initial low state. In the next frame IVID-GATE is directed to commence its operation as described above. Therefore, after frame 3 of the *ACQUIRED SPECTRA* block diagram executes, IVID-MASK and IVID-GATE are performing as shown in Figure 29. Note that the transition of IVID-GATE from high to low is not synchronized with any clock but the transition from low to high is synchronized with IVID-MASK and IVID-DATA. In Figure 29 the duty cycle of IVID-MASK has been modified for clarity. This figure also shows when IVID-REQ is enabled.



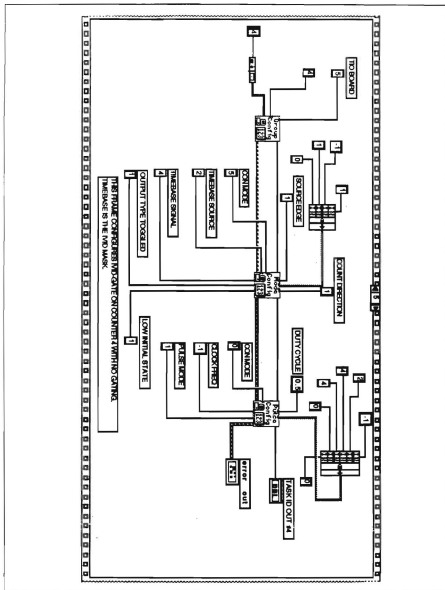


Figure 28. Frame 5 of the SubVI TIO CLOCKS.

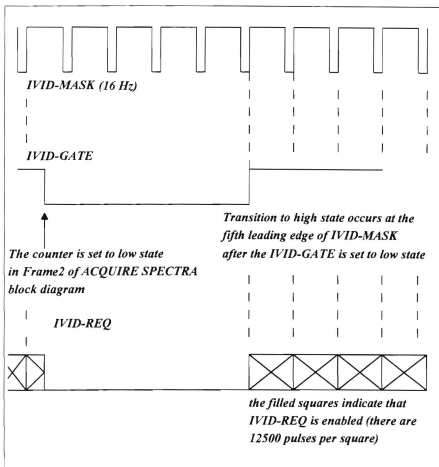


Figure 29. Timing Diagram for IVID-MASK, IVID-GATE and IVID-REQ.

The 200 KHz clock IVID-REQ is configured in frame 6 of the subVI *TIO CLOCKS* which is shown in Figure 30. IVID-REQ is generated on Counter 7 and uses

IVID-TIM for a timebase and IVID-GATE for its gate. The initial state of IVID-REQ is low for a duration of one timebase period followed by the high state that counts four timebase periods. Figure 31 displays the timing between IVID-REQ, IVID-GATE and overall timebase. As described above, when IVID-GATE undergoes a leading edge transition, IVID-REQ begins counting. This clock, IVID-REQ, is used for the handshaking of the NB-DIO-32F board. During each low-to-high transition the NB-DIO-32F will acquire one bit of data. This procedure is explained below along with the configuration and the operation of the digital I/O interface.

The last signal is the IVID-START(TEST) which is generated in frame 7 of *TIO CLOCKS* block diagram which is shown in Figure 32. Although this signal is required by the ISAAC data acquisition box, it is not required for our testing. Therefore, it is replaced by the IVID-TEST which is a clock of variable frequency. IVID-TEST simulates IVID-DATA giving the opportunity to test the *ACQUIRE SPECTRA* program. IVID-TEST is generated on Counter 9. It uses IVID-CLK for a timebase and line A0 for its gate with high level gating mode.

After all these signals are either configured or set to run, the last frame of *TIO-CLOCKS*, frame 9 shown in Figure 33, sets line A0 in a digital high state. This initiates the operation of IVID-STB, IVID-MASK and IVID-TEST. Figure 34 shows these three signals in connection with their gate, line A0, and their timebase, IVID-CLK. In this figure IVID-TEST is shown to have 100 KHz frequency.

With the execution of the last frame of subVI *TIO CLOCKS*, frame 1 of *ACQUIRE SPECTRA* block diagram is completed. Frames 2 and 3 follow. The operation of those two frames was described above in the generation of the signal IVID-GATE.

Frames 1,2 and 3 of *ACQUIRE SPECTRA* block diagram have so far been analyzed. As soon as frame 3 is executed, the counters count in the mode described above. Below, the configuration of the NB-DIO-32F I/O board, frame 0, and the data acquisition and conversion process, frame 5, are examined.



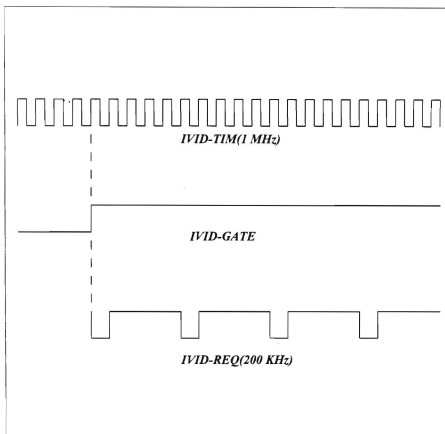


Figure 31. Timing Diagram for IVID-TIM, IVID-GATE and IVID-REQ.





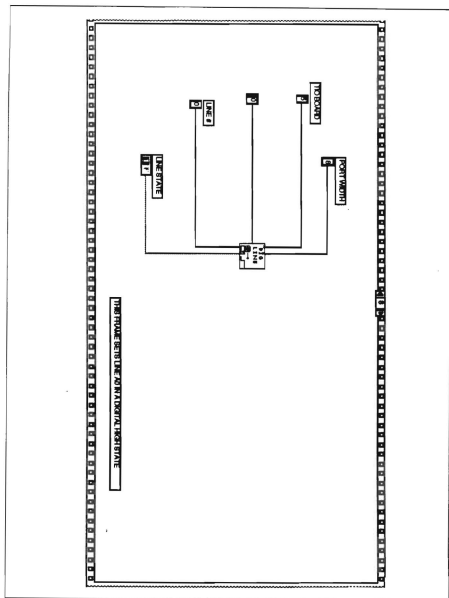


Figure 33. Frame 8 of the SubVI *TIO CLOCKS*.

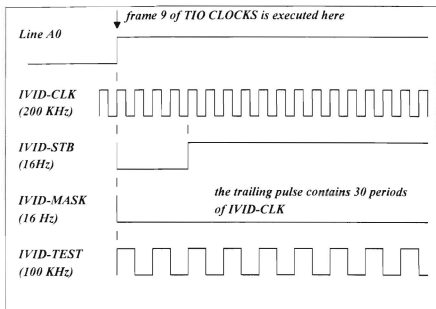


Figure 34. Timing Diagram for IVID-STB, IVID-MASK and IVID-TEST in Relation to Line A0.

## 2. NB-DIO-32F I/O Interface Configuration

Figure 35 shows frame 0 of the *ACQUIRE SPECTRA* block diagram. This frame uses a simple VI to configure port A of the NB-DIO-32F as an input port. The least significant bit of the port receives the signal IVID-DATA. Port A is configured for leading edge handshaking and active high acknowledges. With this configuration, the port acquires data on every rising edge of the signal applied at the REQ 1 pin. Recall that this signal is the IVID-REQ. Port A is configured to make 12288 reads, as many as the data bits carried by IVID-DATA for every pulse of IVID-STB. The VI of this frame also allocates a buffer to hold the scans as they are read. Finally, the VI produces a *TASK ID* that is transferred through a sequence local to frame 5.



### 3. Data acquisition-Transformation Procedure

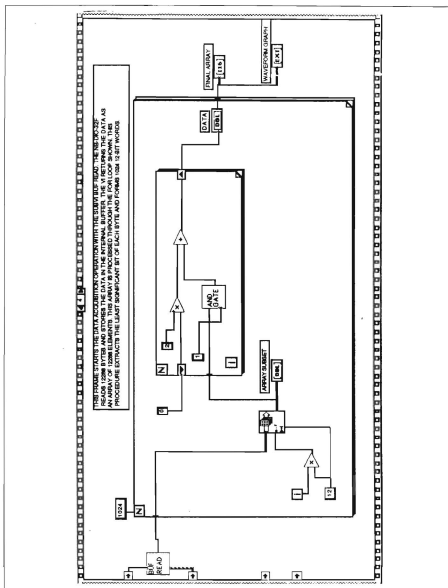
The last frame of the sequence structure of *ACQUIRE SPECTRA* block diagram, frame 5, is shown in Figure 36. This frame contains a subVI named *BUF READ*, which commences the data acquisition operation, and a *for loop* that transforms the 12288 serial bits into an array of 1024 numbers. Each number has 12 bits and represents the intensity received from one of the 1024 photodiodes of the ISAAC detector.

#### a. SubVI *BUF READ*

This subVI receives the *TASK ID* from the VI used in frame 0 where the configuration of the NB-DIO-32F took place. The block diagram of *BUF READ* is shown in Figure 37. *BUF READ* starts the data acquisition operation so that port A reads 12288 scans. The data are stored in an internal transfer buffer. When the data acquisition operation is completed, the subVI returns an array of 12288 elements. Each element is an 8-bit number and each one of those bits represents the value read from one of the eight lines of port A. A schematic representation of this array is shown in Figure 38.

The signal IVID-DATA will be connected to the line DIOA0 which is the least significant bit of this port. The rest of the lines are not connected. Therefore, these seven most significant bits are interpreted by the board as 1 ( digital high state ). As a result, the 8-bit numbers are either 254 or 255 depending on the value of the least significant bit.

The array in Figure 38 is processed in order to extract the least significant bit of each element. Next, these bits are ordered in groups of 12. There are 1024 such groups. The first group of twelve, namely the first twelve bits of IVID-DATA, is the data from the first pixel, the second group from the second pixel and so on. When all this ordering is done, the final output is an array of 1024 12-bit elements. This so-called serial-to-parallel conversion is explained next.





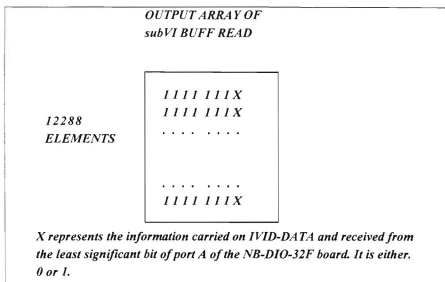


Figure 38. Output Array of BUF READ.

#### ***b. Serial-to-parallel Conversion***

The serial-to-parallel conversion takes place in frame 5 of *ACQUIRE SPECTRA* block diagram as shown in Figure 36. The conversion consists of two nested loops. The array output of *BUF READ* is wired into the outer loop which is repeated 1024 times. In this loop the array of 12288 elements is divided into groups of 12 elements. Each group or array subset enters the inner loop. This second loop uses auto-indexing so that it loops as many times as the number of the elements of the array subset - in this case 12. In addition, a shift register is used as a local variable that feeds values from one iteration to the next. The initial value of the shift register is 0.

The inner *for loop* contains the subVI *AND GATE*. The block diagram of this subVI is shown in Figure 39. *AND GATE* performs the Boolean AND operation on the 8 bits of the element with the number 1. The Boolean AND operation is shown in Figure 40. Each element of the array subset has the form 1111 111X, as shown in

Figure 36, where  $X$  is either 0 or 1. The AND operation of this number with number 1 yields the binary number  $X$  as illustrated in Figure 41.

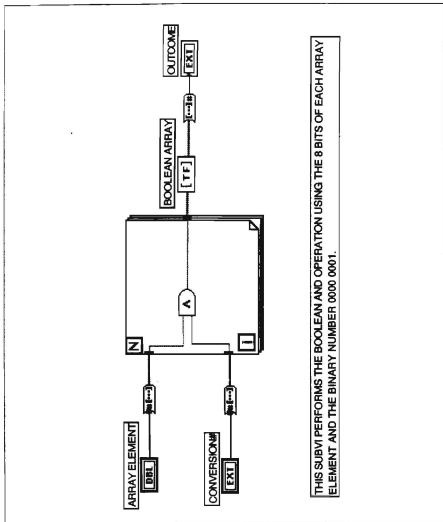


Figure 39. The Block Diagram of the SubVI *AND GATE*.



| <i>A</i> | <i>B</i> | <i>A AND B</i> |
|----------|----------|----------------|
| 0        | 0        | 0              |
| 0        | 1        | 0              |
| 1        | 0        | 0              |
| 1        | 1        | 1              |

Figure 40. Boolean AND Operation.

|                                    |                              |
|------------------------------------|------------------------------|
| <i>1 1 1 1 1 1 1 X<sub>1</sub></i> |                              |
| <i>0 0 0 0 0 0 0 1<sup>1</sup></i> | <b>BOOLEAN AND OPERATION</b> |
| <hr/>                              |                              |
| <i>0 0 0 0 0 0 0 X<sub>1</sub></i> |                              |

Figure 41. First Array Subset Element AND the Number 1.

This value, *0 0 0 0 0 0 0 X<sub>1</sub>*, is added to the initial value of the shift register which is 0. Then it is returned through the shift register to the beginning of the loop. This number is then multiplied by 2 giving the result *0 0 0 0 0 0 X<sub>1</sub> 0*.

Next, the second element of the array subset enters the *for loop* where it goes into the subVI *AND GATE* which produces the number *0 0 0 0 0 0 0 X<sub>2</sub>*. This number is added to the local variable *0 0 0 0 0 0 X<sub>1</sub> 0*. The sum is *0 0 0 0 0 0 X<sub>1</sub> X<sub>2</sub>* and this is shown graphically in Figure 42.

$$\begin{array}{r}
 0\ 0\ 0\ 0\ 0\ 0\ X_1\ 0 \\
 0\ 0\ 0\ 0\ 0\ 0\ 0\ X_2\ + \\
 \hline
 0\ 0\ 0\ 0\ 0\ 0\ X_1X_2
 \end{array}$$

Figure 42. Addition of the Second Output of *AND GATE* and the Shift Register Value.

This number becomes the new value of the shift register with  $X_1 X_2$  being the first two bits of information. This process is repeated a total of twelve times, once for each element of the array subset. As soon as the last iteration is executed, the loop returns the data in the form  $X_1 X_2 X_3 X_4 X_5 X_6 X_7 X_8 X_9 X_{10} X_{11} X_{12}$ . The most significant bit is the very first piece of information carried by the IVID-DATA signal. This process is repeated 1024 times, once for each array subset that the outer loop produces. The final output will be an array of 1024 elements. Each element will be a 12-bit number representing the information received from the corresponding pixel of the ISAAC detector. The form of this array is depicted in Figure 43.

*FORM OF FINAL ARRAY OF ACQUIRE  
SPECTRA PROGRAM*

*first bit of data*

X XXXX XXXX XXXX  
XXXX XXXX XXXX

XXXX XXXX XXXX *12288*

*last bit of data*

### C. GSE INTERFACE-FUTURE CONSTRUCTION OF A GSE BOX

74

| PIN #       | CONNECTED TO PINS #                       |
|-------------|---|
| 29 (FOUT 1) | 15 (SOURCE 6), 18 (SOURCE 7)              |
| 30 (FOUT 2) | 4 (SOURCE 2), 7 (SOURCE 3), 24 (SOURCE 9) |
| 35 (A0)     | 5 (GATE 2), 8 (GATE 3), 25 (GATE 9)       |
| 9 (OUT 3)   | 10 (SOURCE 4)                             |
| 12 (OUT 4)  | 19 (GATE 7)                               |

Table 10. Connections between the Pinouts of NB-TIO-10 board.

| NB-TIO-10 PIN # | CONNECTED TO NB-DIO-32F PIN # |
|-----------------|-------------------------------|
| 20(OUT 7)       | 33(REQ 1)                     |
| 26(OUT 9)       | 37(DIOA0)                     |
| 33(GND)         | 30(GND)                       |

Table 11. Connections between the NB-TIO-10 and the NB-DIO-32F Boards.

The only remaining step is the construction of a GSE interface box. This box will connect the J301 connector of the ISAAC data acquisition box with the GSE data acquisition boards. By this means, the GSE interface will simulate the ARGOS CE box connector, as shown in Figure 17. This will allow testing of the ISAAC spectrograph prior its flight. A schematic representation of this GSE box is shown in Figure 44. It requires three 50-pin female connectors, two from one side and one from the other side. As shown in Figure 44, the two GSE boards and the J301 connector will be connected to the three female pin connectors. Inside the GSE box several connections must be made

between the three connectors. The NB-TIO-10 and the NB-DIO-32F boards can be connected as described above in Tables 10 and 11. The only difference is that the output of Counter 9, which was the IVID-TEST during testing, now becomes the IVID-START. This line (pin 26) should be connected to the IVID-START on the J301 connector. The rest of the J301 connections are shown in Table 12.

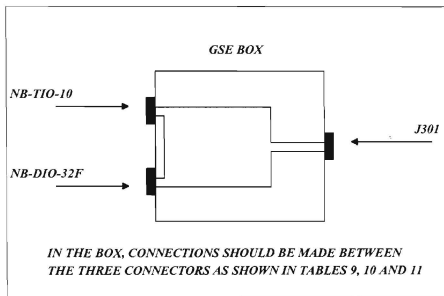


Figure 44. Schematic Representation of a Future GSE Box.

| PIN # OF J301  | CONNECTED TO PIN # OF NB-IIG-10 | CONNECTED TO PIN # OF NB-DIO-321 |
|----------------|---------------------------------|----------------------------------|
| 14(IVID-START) | 26(OUT 9)                       |                                  |
| 16(IVID-STB)   | 6(OUT 2)                        |                                  |
| 32(IVID-DATA)  |                                 | 37(DIOAO)                        |
| 48(GND)        |                                 | 32(GND)                          |
| 49(IVID-CLK)   | 30(FOUT 2)                      |                                  |

Table 12. Connections between the J301 Connector and the GSE Boards.



## V. RESULTS-SUMMARY OF THE GSE

### A. RESULTS

The actual flight instrument is not yet available for testing. Nevertheless, the operation of the GSE was tested. The timing signals that the *ACQUIRE SPECTRA* program generates were displayed on an oscilloscope. It was confirmed that the signals, especially IVID-CLK, IVID-REQ and IVID-STB, are synchronized as designed.

As mentioned in Chapter IV, IVID-START was not needed for testing purposes. As a result this signal was used to simulate data from ISAAC. When used in this way this signal is referred to as IVID-TEST. This simulation provides the opportunity to check the data acquisition process and the serial-to-parallel conversion. Recall that IVID-TEST is synchronized with the request signal of the NB-DIO-32F board, IVID-REQ. Several trials were made with different frequencies of IVID-REQ. IVID-TEST was given half the frequency of IVID-REQ each time. The relation between the two signals is shown in Figure 45. Recall that data are acquired on every rising edge of IVID-REQ so that the final array that the *ACQUIRE SPECTRA* program returns should have elements of the binary form *1010 1010 1010*. For frequencies of IVID-REQ up to 40 KHz the final array of the program contains 1024 elements that are all the same number: 2730, which is the binary number *1010 1010 1010*. This indicates that the data acquisition process and the serial-to-parallel conversion are operating with satisfying results at low request line frequencies.

Unfortunately, above 40 KHz the GSE does not operate correctly. The required frequency of IVID-DATA is 200 KHz. In order to test this frequency, IVID-REQ was set to 200 KHz and IVID-TEST to 100 KHz frequency. The form of the final array at this frequency was not the *1010* pattern as expected. Instead the bit pattern appeared to be random. Since the conversion process performed well at low frequencies, we conclude that the Quadra 650 and the NB-DIO-32F may not be able to correctly acquire high frequency data. The GSE programs were sent to National Instruments, Inc. Data



acquisition personnel of the company ran the programs on their hardware and observed the same results as above. The company's staff are still trying to identify the reasons for the inability of the hardware to acquire high frequency data.

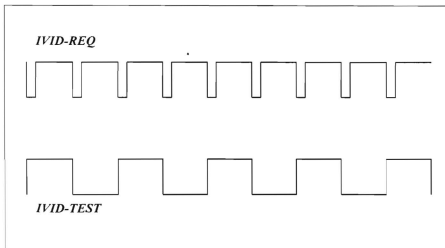


Figure 45. Relation between IVID-REQ and IVID-TEST.

## B. SUMMARY OF THE GSE

This thesis presents the development of a GSE that allows testing of the ISAAC spectrograph prior to its flight. The objectives of the ISAAC spectrograph along with the relative physics background were discussed. The software package and the two GSE boards were presented. In addition, the GSE programs were detailed. In particular, the method by which the GSE generates the signals, that simulate those that the spectrograph will receive from the ARGOS satellite bus, was explained. The data acquisition process and the serial-to-parallel conversion were detailed. Moreover, a description of a potential future construction of a GSE box was given. Finally, some incompatibilities between the hardware and the software were identified.

### **C. FUTURE WORK**

There is more work required to be done following the development of the GSE. First and foremost, the incompatibilities mentioned above need to be resolved. One possible solution is to use a different computer. Thesis opportunities will include construction of the GSE interface box. Upon completion of the ISAAC data acquisition box by NRL, this flight unit must be tested using the GSE. Finally, following the launch of the satellite there will be many opportunities for data analysis.



## LIST OF REFERENCES

- Anderson, D.E., Jr. and Meier, R.R.:1983, 'Determination of Atmospheric Composition and Temperature from the UV Airglow', *Planetary Space Sci.* 33, 1179.
- ARGOS *Comprehensive Design Review*, Rockwell International and Naval Research Laboratory, 17 November 1993.
- Barth, C.A. and F.G. Eparvier, "A Method of Measuring the Temperature of the Lower Thermosphere," *J. Geophys. Res.*, 98, 9437-9441, 1993.
- Cleary, David D., *Analysis of Nitric Oxide FLuorescence Bands from High Latitude Rocket Observations of the Thermospheric Dayglow*, Ph. D. Dissertation, University of Colorado, 1985.
- Eisberg, Robert and Robert Resnick, *Quantum Physics of Atoms, Molecules, Solids, Nuclei, and Particles*, Second Edition, John Wiley & Sons, 1985.
- Hedin, A.E.:1987, 'MSIS-86 Thermospheric Model', *J. Geophys. Res.* 92, 4649.
- Heinz, O., and Olsen, R.C., *Introduction to the Space Environment*, Naval Postgraduate School, 1994.
- Hinteregger, H.E., Fukui, K., and Gilson, B.R.:1981, 'Observational, Reference and Model Data on Solar EUV from Measurements on AE-E', *Geophys. Res. Letters* 8, 1147.
- LabVIEW Tutorial for Macintosh, Version 3.1, Part Number 320590B-01, National Instruments Corporation, September 1994.
- LabVIEW User Manual for Macintosh, Version 3.1, Part Number 320590B-01, National Instruments Corporation, September 1994.
- LabVIEW 2 Labdriver VI Library Reference Manual, Version 4.2, Part Number 320249-01, National Instruments Corporation, February 1991.
- LabVIEW 2 User Manual, Part Number 320244-01, National Instruments Corporation, January 1993.

MacQuarrie, J.A., *A Ground Support Electronic Interface for the Ionospheric Spectroscopy and Atmospheric Chemistry (ISAAC) Spectrograph*, Master's Thesis, Department of Aeronautics and Astronautics, Naval Postgraduate School, December, 1994.

NB-TIO-10 User Manual, Part Number 320309-01, National Instruments Corporation, July 1993.

NB-DIO-32F, User Manual, Part Number 320095-01, National Instruments Corporation, May 1988.

## INITIAL DISTRIBUTION LIST

1. Defense Technical Information Center.....2  
     Cameron Station  
     Alexandria, Virginia 22304-6145
  
2. Library, Code 52.....2  
     Naval Postgraduate School  
     Monterey, California 93943-5101
  
3. Dr. William B. Colson.....1  
     Physics Department, Chairman PH  
     Naval Postgraduate School  
     Monterey, CA 93943-5000
  
4. Dr. D.D. Cleary.....3  
     Physics Department, PH/CI  
     Naval Postgraduate School  
     Monterey, CA 93943-5000
  
5. Dr. Suntharalingam Gnanalingam.....1  
     Physics Department, PH/Gm  
     Naval Postgraduate School  
     Monterey, California 93943-5000
  
6. LTJG. Fragiskos Leloudas.....2  
     Pelloponisou 11  
     Ilisia, 15771  
     Athens, Greece







ODDLEY KNOX LIBRARY



3 2768 00314627 5 -